ENGINEERING RESEARCH INSTITUTE
UNIVERSITY OF MICHIGAN
ANN ARBOR

UPPER AIR RESEARCH PROGRAM

REPORT NO. 3

DYNAMIC PROBE MEASUREMENTS IN THE IONOSPHERE

BY

GUNNAR HOK

N. W. SPENCER

A. REIFMAN

W. G. DOW

Project M824

AIR MATERIEL COMMAND
AIR FORCE CAMBRIDGE RESEARCH LABORATORIES
CAMBRIDGE, MASSACHUSETTS

ACKNOWLEDGEMENTS

The authors gratefully acknowledge the very important contributions to the success of this investigation made by the past and present members of the upper atmosphere research group of the Department of Electrical Engineering at the University of Michigan. The construction of the equipment and the preparation for the flights, as well as the reduction of the data from the telemetering records, were possible only through the wholehearted cooperation of everybody involved in this work.

TABLE OF CONTENTS

LIST OF FIGURES

ABSTRACT

A method is discussed in this report whereby data on the characteristics of the E-layer of the ionosphere may be obtained. A bipolar exploring electrode system is flown on a rocket and its volt-ampere curves at various altitudes interpreted in terms of the concentration and energy distributions of ions and electrons. Such a bipolar probe consists of two isolated, as far as possible, noninteracting electrodes connected to the two terminals of a variable-voltage source; it is particularly suitable for immersion in an ionized medium without any convenient reference electrode, e.g., in an electrodeless discharge, a decaying plasma, or the ionosphere.

In the first part of this paper a brief review is given of our present knowledge and ideas about the E-layer and it is attempted to postulate a simple "model" E-layer with a minimum number of parameters. In the second and third parts Langmuir's probe theory is reviewed and its application to the ionosphere and to a geometry realizable on a rocket is discussed in detail, as well as numerical and graphical methods for determining the constants of the model ionosphere from probe data.

The fourth part describes the first rather crude experiments with bipolar probes on rockets. The reduction of the data has met with considerable difficulty. The main reasons are held to be the rather unfavorable geometry and the disturbances caused by the motion of the rocket through the atmosphere. It has not been possible to work out a complete and unambiguous interpretation of all the data obtained during the flight in terms of the concentrations and energies of the ions and electrons. A detailed discussion of what is considered the most plausible interpretation is included.

This tentative interpretation requires that the concentration of the negative ions be considerably larger than the concentration of the electrons.

The prospects of obtaining unambiguous results by improved probe design are considered at length and are found to be encouraging. To arrive at a conclusion in this respect, based on the experience gained during the preliminary experiments, is held to be the main objective of this report.

DYNAMIC PROBE MEASUREMENTS IN THE IONOSPHERE

INTRODUCTION

Most of our knowledge of the properties of ionized gases has been derived from experiments with electrical discharges through gas-filled tubes. In the study of the ionized layers of the upper atmosphere it is natural to try to draw whatever parallels are possible between the behavior of these layers and the plasma in a gas-discharge tube, with due regard for the considerable difference in ion densities and processes of ionization and recombination. Early suggestions in this direction were made by Tonks.[1]

When the V-2 rocket became available for upper atmosphere research after the end of the second World War the opportunity arose to apply to the exploration of the lower ionosphere the probe method developed by Langmuir and his associates for study of the properties of the plasma in a gas-discharge tube.[2,3] The single-probe technique used in gas-discharge tubes had to be modified to a differential arrangement involving two collectors with a controlled difference of potential but with an absolute potential free to assume any equilibrium value required by the total rate of collection of positive and negative particles. In connection with a contract between the Air Materiel Command of the U. S. Air Force and the University of Michigan concerning instrumentation of

V-2 rockets for measuring pressure, temperature, ion density, and ion energy in the upper atmosphere, one of the present authors, W. G. Dow, suggested this bipolar variable-voltage-probe method for the study of the characteristics of the lower ionosphere. Such probes of early and not too adequate design have been in operation on three successful V-2 flights, in November, 1946, in February, 1947, and in December, 1947, respectively. The first flight proved that the scheme could work, although scale ranges and other details had not been predicted accurately enough to furnish useful data. The December 1947 flight gave a continuous record of well defined probe curves for altitudes between 80 and 103.5 km. Attempts have been made to calculate from these data at least rough approximations of ion concentration and electron energy. The set of probe characteristics deviates considerably from what would be predicted from probe theory applied to a thin plasma in temperature equilibrium at 250-300°K. The main reasons are believed to be:

1. The shape of the collectors does not approximate closely enough any of the ideal geometries for which the current collection is known.

2. The ion sheaths of the two collectors overlap, so that a complicated interaction takes place between them.

3. The air flow about the rocket upsets the thermal equilibrium in the vicinity.

Despite these discrepancies we believe that the experience gained during these flights and during the analysis of the collected data point the way to improved design and promise valuable data from future flights.

In this report we shall begin with a summary of the properties of the lower ionosphere as deduced from observations of various kinds as

well as from calculations based on established physical laws. We shall attempt to specify the state of the ionized air at any point in space in terms of a minimum number of measurable quantities.

The next task is to relate these quantities to the observed volt-ampere curves of a bipolar probe and to estimate the errors and disturbing influences produced by other previously neglected factors and processes. Optimum design of the collector surfaces and graphical and numerical methods for the computation of the characteristics of the E-layer will also be discussed at length.

Finally, the results obtained during the December 1947 flight will be analyzed and the difficulties referred to above will be investigated. Necessary modifications of the computation procedure are introduced and the final result presented. Tentative interpretations are given for unexpected behavior of the probe current, particularly during descent.

THE E-LAYER OF THE IONOSPHERE

At an altitude of 100-105 km the composition of the atmosphere is believed to change rather abruptly: below this altitude the oxygen appears nearly exclusively in molecular form; above, the atomic oxygen predominates.[4] When the radiation from the sun reaches the molecular oxygen which has a considerably lower ionizing potential than the atmospheric layers above it, an increased photo-ionization is to be expected. The resulting ion concentration reaches a steady state when the loss of ions due to recombination and diffusion equals the rate of photo-electron ionization. A generally acceptable recombination process to explain the concentrations observed by radio-propagation measurements has not with certainty been established as yet.[5,6] As to the

importance of diffusion in the ionosphere, a widely spread opinion seems to hold diffusion a negligible item in the ion-balance equation of the E-layer.[7,8]

The ratio of the concentrations of negative ions and electrons in the E-layer has in general been assumed to be negligible. Theoretical calculations by Bates and Massey gave an order of magnitude of this ratio of a few tenths of one per cent. Several independent experimental indications have recently been found of a very much higher ratio. The relatively long life of each free electron enables it, despite the low gas pressure, finally to attach itself to a gas molecule, but the abundance of photons of sufficient energy for photodetachment was considered to make it improbable that it will remain attached an appreciable part of its life. The probe measurements are not accurate enough to give an independent estimate of the electron concentration. This ratio, therefore, enters the considerations in this report only in the comparison between the positive ion concentration obtained from the probe data with the electron density determined by radio-propagation methods.

The gas temperature at the altitude of the E-layer is estimated to be 250-300°K. It is the predominant opinion among ionosphere physicists that temperature equilibrium is at least to a rough approximation prevalent in the E-layer. It should be pointed out, however, that a number of phenomena have been continuously observed which constitute disturbances of the equilibrium. Such phenomena are steady winds of velocities in the range 50 to 100 m/sec, random winds of 2 to 3 m/sec, formation and movement of ion clouds, etc.[9,10] In the interpretation of rocket data it should also be remembered that the presence and motion of the rocket itself cause a disturbance in its immediate vicinity. It is thus not to be

expected that the ion and electron energies should under all conditions correspond to the temperature of the air at rest.

Introduction of the concepts of ion and electron temperatures implies the assumption of a Maxwell-Boltzmann distribution of ion and electron energies. The justification for this assumption may be questioned, particularly as regards the electrons. At ionization the lion's share of the surplus energy of the photon becomes kinetic energy of the electron. If this energy is lost in collisions in a small fraction of the lifetime of the electron, the velocity distribution of the electron will be very nearly Maxwellian. The electron temperature will be equal to the gas temperature unless a continuous source of energy, like an impressed electric field, exists. Similarly, a recombination process that favors a certain energy range will cause only insignificant deviations from the Maxwellian velocity distribution, if the rate of recombination is insignificantly small compared with the collision rate.

The characteristics of the E-layer at a certain point should then be stated in terms of the positive-ion density, the negative-ion density, the electron density, the air pressure, and the equilibrium temperature as a function of the altitude. If there are any reasons to doubt the temperature equilibrium, the gas temperature, ion temperatures, and electron temperature have to be specified separately.

Experimental observations of the maximum electron concentration in the E-layer are continuously made by radio-propagation measurements. These observations give the altitude of this maximum as varying between 100 and 120 km. Pressure measurements have been made from rockets at this altitude, and the temperature has been calculated by means of the barometric equation under the assumption of constant composition of the

air.[11,12] Direct temperature observations by sound-velocity measurements have been attempted, but no data have so far been obtained up to and above 100-km altitude.

Some experiments performed in England to explore the "Luxembourg effect", i.e., the intermodulation between strong radio signals in the E-layer, are of particular interest because the electron temperature is a rather important parameter in the theory of this effect.[13] The quantitative agreement between observations and calculations based on assumed temperature equilibrium is reasonably good, giving rather strong support to the assumed temperature equilibrium, at least in the lower strata of the E-layer.

The correct approach to an experimental investigation like the present one is, of course, not to rely on any a priori assumptions of this kind but to leave it to the probe data to give information as to the energy distribution of the ions and electrons. However, the problem involves so many variables connected by transcendental relations that we should take on an unnecessarily severe handicap if we did not make critical use of all previous work in the field, continuously checking its compatibility with our observations, if possible, as we go along.

The undisturbed E-layer in the ionosphere is assumed to be a region free of electric fields where in each volume element, on the average, the concentration of positive charge equals that of negative charge. In the vicinity of a conducting body immersed in this "plasma", however, such a state cannot be maintained. If the body has a negative potential with respect to the plasma, a unipolar, positive-space-charge sheath is formed at its surface containing very few electrons and negative

ions but an appreciable density of positive ions. Outside the sheath there will be a region of ambipolar diffusion which continuously replaces the ions and electrons that pass through the sheath and are collected by the body.

In a quantitative study of the equilibrium state in the vicinity of the conductor the first step is to derive the relations between sheath thickness, across-the-sheath potential, and current collected, on the one hand, and the particle densities and energies at the sheath edge, on the other. Since these densities and energies are not those of the undisturbed plasma it is necessary to consider the variations of these quantities in the region of ambipolar diffusion. At the sheath edge this region is subject to a constant drain of ions and electrons. Since the medium is viscous a concentration gradient is required in the diffusion region. Also, because of the more rapid diffusion of electrons, a weak electric field must exist, retarding the negative particles and accelerating the positive ions. At the sheath edge, therefore, the concentrations of all the charged particles must be expected to be lower and the positive-ion energy higher than in the undisturbed plasma.

In the next sections the quantitative relations between the current collection and potential of a conductor and the characteristics of the plasma in which it is immersed will be discussed. Experimental and computational procedures will be described by means of which these characteristics can be determined.

REVIEW OF THE PROBE THEORY

A. Single Probe

When an electrode immersed in an ionized gas is brought to a potential different from that of the gas, a space-charge region or "sheath" forms around it of opposite polarity to the potential of the electrode. If the gas pressure is so low that the probability is small for an ion or electron entering the sheath to collide with gas molecules before it reaches the electrode, the current to the electrode can be calculated in terms of the dimensions of the sheath, the velocity distribution of the ions and electrons arriving at the sheath boundary, and the total potential differences across the sheath. The current reaching the electrode is independent of the actual distribution of potential in the sheath, with certain mild reservations. The thickness of the sheath and the potential distribution inside are determined by space-charge considerations rather than by the initial velocities of the ions and electrons and the potential difference between the collector and the gas.

Consider a cylinder or wire whose length l is large compared to its radius r so that axial space variations can be neglected. Assume that the composition of the ionized gas is uniform about the collector and that the ion velocities are random. The sheath will then be a circular cylinder concentric with the collector; let its radius be $\underline{a}$ meters. Considering the ions of one particular sign only, let N be the number per unit volume in a small element of volume $d\tau$ bordering the sheath. In a plane normal to the axis let u be the radial and v the tangential component of velocity of an ion, u being counted positive when directed toward

the center. Then, if

$$Nf(u,v)du\ dv\ d\tau$$

is the number of ions in $d\tau$ that can be expected to have velocity components u and v lying in specified ranges u to u + du and v to v + dv, the total number of ions expected to cross the sheath edge with velocities within the given limits in unit time will be

$$2\pi\ a\ N\ u\ f(u,v)\ dudv \tag{1}$$

On multiplying (1) by the ionic charge e and the length ℓ of the electrode and integrating between the proper limits, the following equation is obtained for the expected value of the total current to the electrode.

$$i = 2\pi\ a\ N\ e \int_{0,u_1}^{\infty} \int_{-v_1}^{v_1} uf(u,v)\ dvdu \tag{2}$$

Here the lower limit of u is to be taken as zero when the collector potential is accelerating, as u_1 when it is retarding. The limits u_1 and v_1 are obtained by applying the laws of conservation of energy and angular momentum to the problem of ion flow to the electrode. The following values are obtained

$$v_1^2 = \frac{r^2}{a^2 - r^2}\ (u^2 + 2\frac{e}{m}V) \tag{3}$$

$$u_1^2 = -2\frac{e}{m}V \tag{4}$$

e = charge of ion

m = mass of ion

V = potential of electrode with respect to the sheath edge, to be taken positive when the electrode attracts ions.

The expected value of the total current I crossing a unit area at the edge of the sheath is

$$I = Ne \int_0^{\infty} \int_{-\infty}^{\infty} u\, f(u,v)\, dv\, du \tag{5}$$

These equations, (2) and (5), give the current to the electrode and the current per unit area at the sheath edge for any distribution of the velocity components u and v.

If the velocity components are assumed to have a Maxwellian distribution the distribution function is

$$f(u,v) = \frac{m}{2\pi kT} \cdot e^{-(m/2kT)\,(u^2 + v^2)} \tag{6}$$

where k is Boltzmann's constant and T is the ion temperature in degrees Kelvin.

When this distribution function is introduced into Eq. (5), the following expression for the expected ion-current density entering the sheath is obtained:

$$I = Ne \sqrt{kT/2\pi m} \tag{7}$$

It is, of course, not strictly correct to assume that this is the current density at the edge of the sheath. Actually, it represents the isotropic current density in a space where the velocity distribution

is everywhere Maxwellian. At the sheath edge, however, the distribution cannot be Maxwellian, since more ions enter the sheath than leave it; in extreme cases all ions that enter the sheath will proceed to the collector, so that no ions leave the sheath. By considering Eq. (7) as the "temperature-limited emission" from the sheath edge we are treating a transport problem as an equilibrium problem, and the result should be regarded as an approximation to be justified by experimental observations.

It is convenient at this point to introduce dimensionless variables for current and potential

$$i_n = \frac{i}{2\pi r \ell I} = \frac{i}{AI} \tag{8}$$

$$\eta = eV/kT \tag{9}$$

where $A = 2\pi r\ell$ = the area of the collector.

From Eq. (2) we now obtain, for an accelerating potential, that is $\eta > 0$,

$$i_n = \gamma \operatorname{erf} \left\{ \frac{\eta}{\gamma^2 - 1} \right\}^{1/2} + e^{\eta} \left[1 - \operatorname{erf} \left\{ \frac{\eta \gamma^2}{\gamma^2 - 1} \right\}^{1/2} \right] \tag{10}$$

For a retarding potential, that is $\eta < 0$,

$$i_n = e^{\eta} \tag{11}$$

Here

$$\operatorname{erf} x = \frac{2}{\sqrt{\pi}} \int_0^x e^{-y^2} \, dy \tag{12}$$

$$\gamma = a/r \tag{13}$$

For a retarding collector potential the current is independent of the sheath radius, and according to Eq. (11) its logarithm is a linear

function of the collector potential, the slope of the line representing this function being e/kT.

For an accelerating potential, the current reaching the electrode depends on the sheath radius, so that another independent relation between i_n, η, and γ is needed to calculate the current. This relation is the equation of space-charge-limited flow in a cylindrical system.

$$i = \frac{8\sqrt{2\pi}\ \varepsilon_o}{9}\sqrt{e/m}\ \frac{\ell V^{3/2}}{r(-\beta)^2} \tag{14}$$

This equation is derived under the assumption that the ions have no random velocity. An approximate correction for a Maxwellian initial velocity distribution of temperature T is obtained by replacing $V^{3/2}$ by $V^{3/2}\,(1 + 0.0247\sqrt{T/V})$. $(-\beta)^2$ is a transcendental function of γ which has been tabulated by Langmuir and Blodgett. In terms of the dimensionless variables introduced in Eqs. (8) and (9) Eq. (14) can be written

$$i_n = \frac{P}{(-\beta)^2}\ \eta^{3/2} \tag{15}$$

where

$$P = \frac{8\ \varepsilon_o\ kT\sqrt{\pi}}{9r^2\ Ne^2} \tag{16}$$

Eqs. (10) and (15) form, with $(-\beta)^2 = f(\gamma)$, a transcendental system that in general can be solved only by numerical or graphical methods. A simple graphical approach makes use of a graph of Eq. (10) in log-log coordinates (Fig. 1). For given values of collector radius r and ion concentration N Eq. (15) will be represented in the same coordinates by a family of straight lines with the slope 3/2. For each γ, the intersection

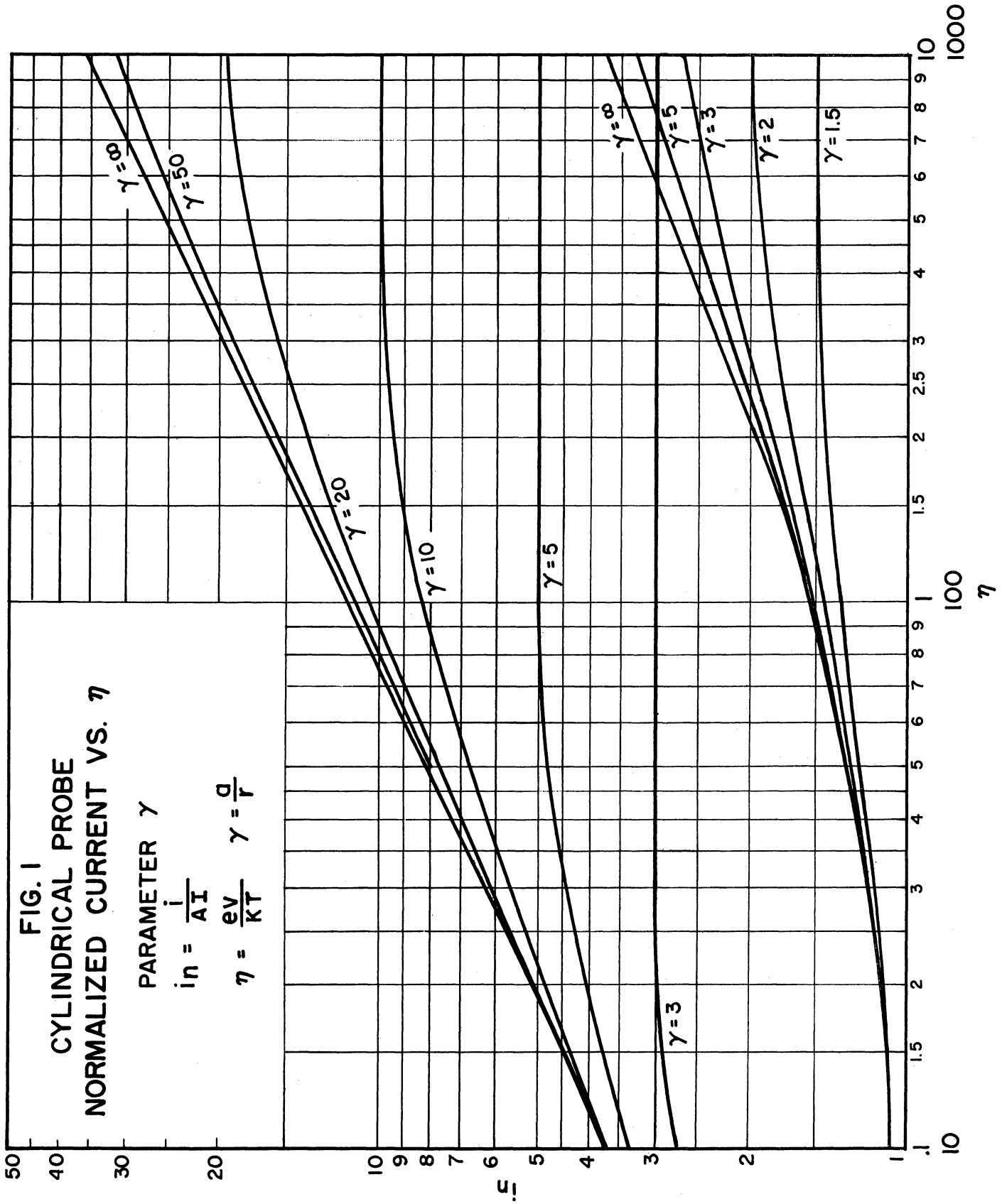
FIG. 1
CYLINDRICAL PROBE
NORMALIZED CURRENT VS. η
PARAMETER γ
$i_n = \frac{i}{AI}$
$\eta = \frac{ev}{KT}$ $\gamma = \frac{a}{r}$
γ=∞
γ=50
γ=20
γ=10
γ=5
γ=∞
γ=5
γ=3
γ=2
γ=1.5
γ=3
i_n
η

between a curve (10) and a line (15) gives a solution to the simultaneous equations and a curve through all these intersections represents the current vs. the voltage for this collector radius and ion concentration.

Numerical calculations of plasma characteristics can often be very much simplified by use of one of two asymptotic forms of Eq. (10). One of these asymptotic relations is represented by the common envelope of the curves, the other by the horizontal asymptotes of the individual curves for large values of η.

Along the envelope the current is unaffected by the space-charge density in the sheath, and the current is said to be limited by the orbital motion of the ions. The current is in this case

$$i_n = \frac{2}{\sqrt{\pi}} \sqrt{1 + \eta} \tag{17}$$

These conditions are obtained for low ion density, small collector radius, or high ion temperature. The quantitative criterion will be given later.

It is seen from Eq. (17) that i_n^2 varies linearly with η, or the square of the collector current with the collector potential. If the slope of the line representing this relation is obtained from experimental data, the ion density can be calculated from Eqs. (17), (7), (8), and (9). Denoting this slope by S amps^2 per volt, we obtain

$$N = \frac{\pi}{Ae} \sqrt{Sm/2e} \tag{18}$$

The intercept of the line on the voltage axis V_o gives the ion temperature

$$T_i = 11600 \cdot V_o \tag{19}$$

This relation is not useful to determine the ion temperature, however, since V_o is usually too small to be measured accurately.

The second asymptotic form of Eq.(10) is obtained for low ion temperature, large ion density, or large collector radius. It is

$$i_n = \gamma \tag{20}$$

In this case the current is entirely unaffected by the orbital motion; all ions that enter the sheath reach the collector. This condition is described as sheath-area-limited current.

When Eq.(20) is combined with Eq.(15) and with the relation between $(-\beta)^2$ and γ, a family of curves is generated with the quantity P as parameter (Eq. 16). In a graph with logarithmic coordinates these curves are over a wide range ($1.5 \leq i_n \leq 100$) nearly identical in shape with the curve representing Eq.(17) but displaced horizontally by an amount determined by P (Fig. 2). This means that in general the volt-ampere curve of

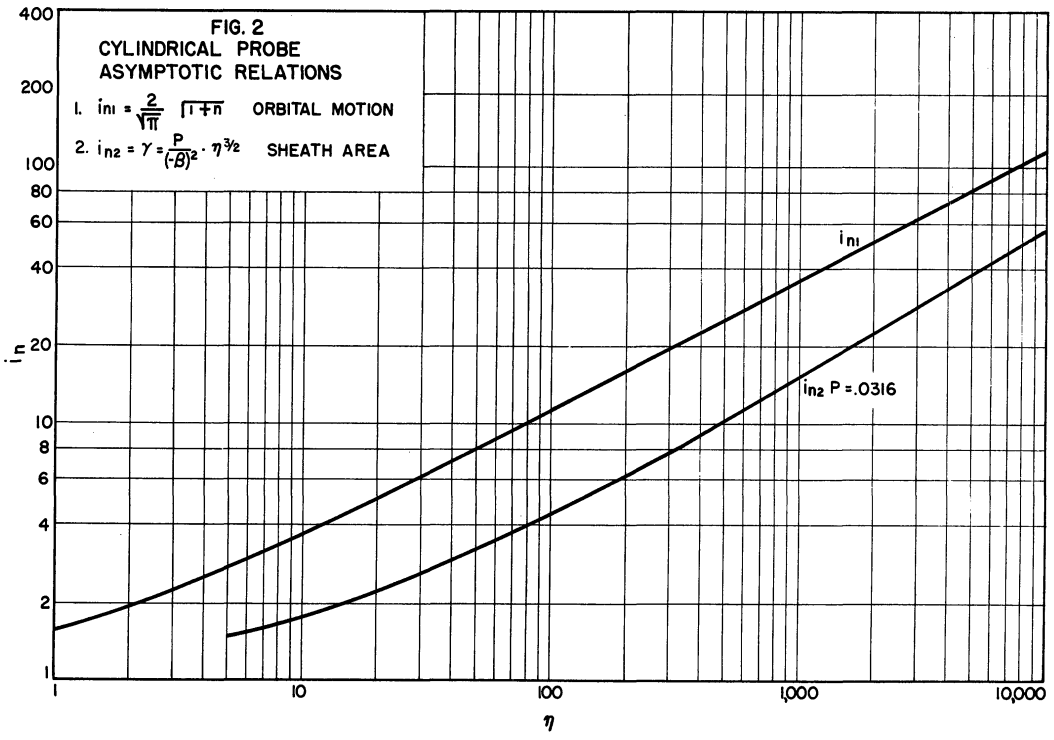

the collector for an accelerating potential can be expressed by the equation

$$i_n \approx 2/\sqrt{\pi}\ \sqrt{1+\mu\eta}\,, \tag{21}$$

where μ is a factor smaller than one. When the current is sheath-area limited, μ is approximately $1.5 \cdot P^{2/3}$. For conditions intermediate between sheath-area-limited and orbital-motion-limited current μ is given by Fig. 3, which has been obtained graphically from Eqs. (10) and (15). The inclined asymptote to the left represents sheath-area-limited current, and the second asymptote $\mu = 1$ represents orbital-motion-limited current. This graph shows clearly what the criteria are for the validity of these two asymptotic solutions. The current is limited by

$$\text{sheath area, if} \quad T/N r^2 \leq 10^{-4} \tag{22}$$

$$\text{orbital motion, if} \quad T/N r^2 \geq 10^{-2}. \tag{23}$$

It should be noted that according to Eq. (21) a plot of i_n^2 vs. η should approximate a straight line, whether the current is limited by orbital motion or not. The slope of the line has a different interpretation if $\mu \neq 1$, and the intercept on the axis is larger than the voltage equivalent of temperature by a factor of $1/\mu$.

Eq. (21) is accurate within 10 per cent over most of the range indicated. The errors increase at the upper end of the range so that the sheath-area-limited current at $i_n = 100$ is actually about 40 per cent larger than the value given by Eq. (21).

The method used for the reduction of data in this report for sheath-area-limited current is based on Eqs. (15) and (20).

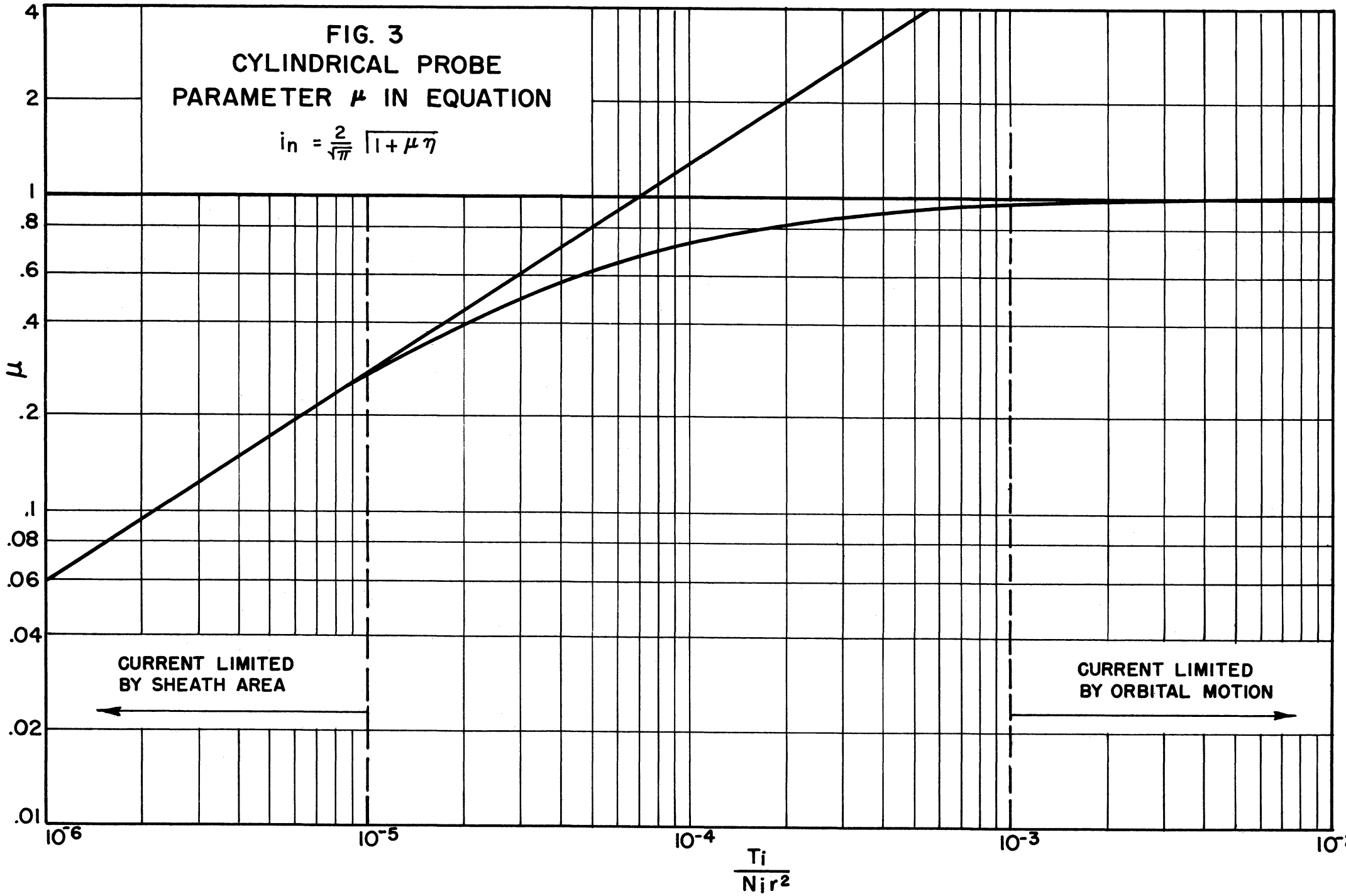
FIG. 3
CYLINDRICAL PROBE
PARAMETER μ IN EQUATION
$i_n = \frac{2}{\sqrt{\pi}} \sqrt{1+\mu\eta}$
μ
4
2
1
.8
.6
.4
.2
.1
.08
.06
.04
.02
.01
CURRENT LIMITED
BY SHEATH AREA
CURRENT LIMITED
BY ORBITAL MOTION
10^{-6}
10^{-5}
10^{-4}
10^{-3}
10^{-2}
$\frac{Ti}{Nir^2}$

Taking the logarithm of both sides in these equations we get

$$\log i_n = \log \gamma = \log P + 3/2 \log \eta - \log(-\beta)^2 \qquad (24)$$

By differentiation

$$d(\log i_n) = d(\log \gamma) = 3/2\, d(\log \eta) - d\left[\log (-\beta)^2\right] \qquad (25)$$

$$\frac{d(\log i_n)}{d(\log \eta)} = \frac{d(\log \gamma)}{d(\log \eta)} = \frac{1.5}{1 + \frac{d \log(-\beta)^2}{d \log \gamma}} \qquad (26)$$

or

$$\frac{d \log(-\beta)^2}{d(\log \gamma)} = 1.5 \frac{d(\log \eta)}{d(\log i_n)} - 1 = 1.5 \frac{idV}{Vdi} - 1 \qquad (27)$$

This quantity can thus be computed from experimental data (coordinates and slope of one point of a current-vs.-voltage curve).

A graph of this quantity as a function of $\gamma = a/r$ (Fig. 4) yields the ratio of sheath radius to collector radius for the point considered. The graph given here is approximate, in that it has been derived from Langmuir's $(-\beta)^2$ by graphical differentiation.

When the resulting value of γ is introduced in (21), (8) and (7), not the ion concentration, but the product of the ion concentration and the square root of the ion temperature is obtained, so that another independent relation involving one or both of these quantities is required.

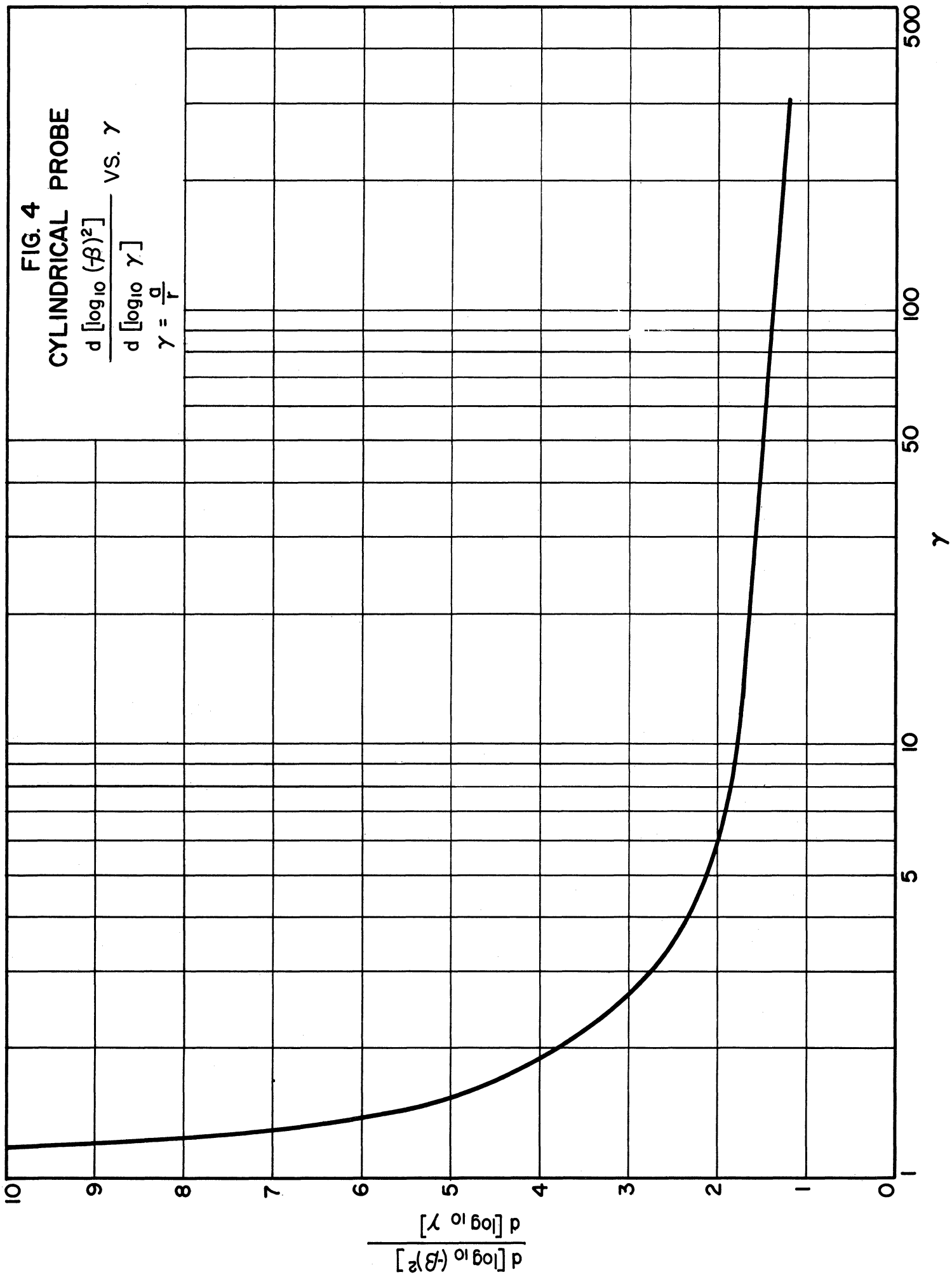
FIG. 4
CYLINDRICAL PROBE
$\frac{d\,[\log_{10}(-\beta)^2]}{d\,[\log_{10}\,\gamma]}$ VS. γ
$\gamma = \frac{a}{r}$
$\frac{d\,[\log_{10}(-\beta)^2]}{d\,[\log_{10}\,\gamma]}$
γ
0
1
2
3
4
5
6
7
8
9
10
1
5
10
50
100
500

Since the plasma contains positive ions, negative ions, and electrons, the collection of all three types of particles determines the volt-ampere curve of a cylindrical probe (Fig. 7, collector No. 1).

However, for large negative collector potential the negative-particle current is negligible, so that the Part A-B on the curve represents positive-ion current alone. If the radius of the probe is so small that the ion current is known to be limited by orbital motion along this part of the curve, the positive-ion density can be calculated from the slope of a line representing the square of the current plotted vs. the potential of the probe (Eq. 18). An extrapolation of the ion current into the range B-C by means of this line makes it possible to separate positive-ion and negative-particle current in this region. If the positive-ion current is known to be sheath-area-limited, the procedure involving Eq. (27) yields the product of the positive-ion concentration and the square root of the positive-ion temperature. According to Eq. (21) the positive-ion current can still be extrapolated in the same way into the region B-C for separation of the negative and the positive-particle currents. The negative-particle current varies so much faster with the potential than the positive-ion current that the approximate character of Eq. (21) introduces a negligible error in the negative-particle current obtained by the extrapolation procedure. The negative-particle current is the sum of the electron current and the negative-ion current

$$i = 2\pi r l \left\{ I_e \cdot e^{eV/kT_e} + I_n \cdot e^{eV/kT_n} \right\} \qquad (28)$$

Since the random current density I (Eq. 7) is directly proportional to the particle concentration N and inversely proportional to the

square root of the particle mass m, the electron component will predominate unless the negative-ion density is very much larger than the electron density. In every case, as long as the negative-ion temperature is equal to the electron temperature, this temperature can be determined from experimental data by measuring the slope of the line representing the equation

$$\log (i_n + i_e) = \frac{eV}{kT_e} + \text{const.} \qquad (29)$$

If the ratio between negative-ion concentration and electron concentration were known, it would theoretically be possible to calculate also these concentrations from the same set of data. Because of the steep exponential variation, however, an extremely accurate knowledge of the potential difference between the gas and the collector is required. For this reason this method is usually not practically useful for determination of negative-ion and electron concentration.

B. Bipolar Probe

When the single-probe circuit cannot be connected to an electrode of fixed potential with respect to the ionized gas, such as the anode or the cathode in a gas-discharge tube under constant operating conditions, a combination of two probes, each connected to one of the terminals of a variable-voltage source, can be used. The application of such bipolar probes to the exploration of the E-layer of the ionosphere is the subject of this report.

The theory of the bipolar probe can be simply derived from the preceding discussion of the single probe. Consider a combination of

two long cylindrical collectors (Fig. 5). Preferably, one of them should have small enough diameter for the positive-ion current to be limited by orbital motion, so that the positive-ion concentration can be determined

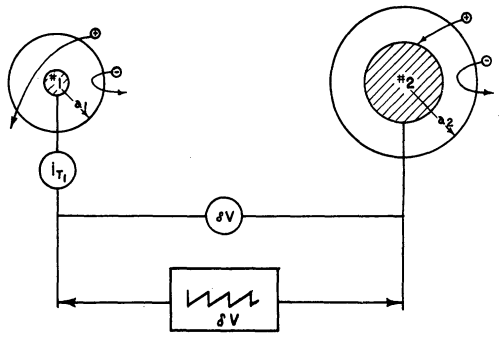

FIG. 5 SCHEMATIC DIAGRAM OF A BIPOLAR PROBE

independently of the positive-ion temperature. A considerably larger second collector has some merits both from practical and theoretical points of view. The ion current to this electrode (No. 2) shall therefore be considered sheath-area-limited. In the following discussion both ions and electrons are assumed to have a Maxwell-Boltzmann energy distribution at the sheath edge.

From the preceding section and Eqs. (7)-(9), (11), (17), and (21) it is seen that the expected values of the total currents to the collectors No. 1 and No. 2, respectively, may be given by

$$i_{T_1} \cong A_1 I_p \cdot \frac{2}{\sqrt{\pi}} \left[\eta_{1p} + 1\right]^{1/2} - A_1 I_e \, e^{\eta_{1e}} - A_1 I_n \cdot e^{\eta_{1n}} \qquad (27)$$

$$i_{T_2} \cong A_2 I_p \cdot \gamma_2 - A_2 I_e \cdot e^{\eta_{2e}} - A_2 I_n \cdot e^{\eta_{2n}} \qquad (28)$$

where

$$I_p = N_p \cdot e \sqrt{\frac{kT_p}{2\pi m_p}} = \text{random positive-ion-current density} \qquad (29)$$

$$I_e = N_e \cdot e\sqrt{\frac{kT_e}{2\pi m_e}} = \text{random electron-current density} \qquad (30)$$

$$I_n = N_n \cdot e\sqrt{\frac{kT_n}{2\pi m_n}} = \text{random negative-ion-current density} \qquad (30a)$$

N_p = concentration of positive ions at outer face of sheath

N_n = concentration of negative ions at outer face of sheath

N_e = concentration of electrons at outer face of sheath

A_1, A_2 = surface areas of collectors No. 1 and No. 2 respectively

$$\eta_{1p}, \eta_{1e}, \eta_{1n}, = -\frac{eV_1}{kT_p}, \quad +\frac{eV_1}{kT_e}, \quad +\frac{eV_1}{kT_n}$$

$$\eta_{2p}, \eta_{2e}, \eta_{2n} = -\frac{eV_2}{kT_p}, \quad +\frac{eV_2}{kT_e}, \quad +\frac{eV_2}{kT_n}$$

T_e, T_p, T_n = electron, positive-ion and negative-ion temperature, respectively

V_1, V_2 = across-the-sheath potentials for collectors No. 1 and 2 respectively, also <u>approximately</u> the potentials of these collectors relative to space potential. Both V_1 and V_2 are always numerically negative.

In regard to the symbols V_1, V_2 and referring to Fig. 6, it is evidently convenient to consider collector potentials as being measured relative to the space potential; therefore, basically, zero potential

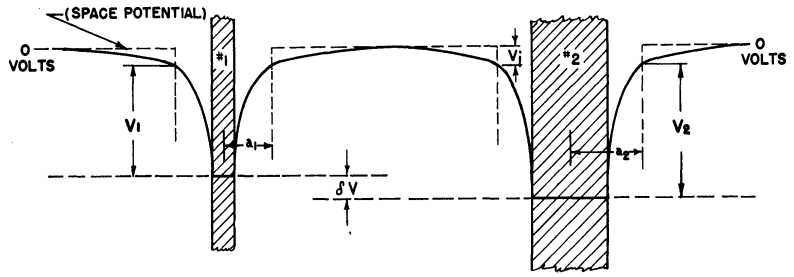

FIG. 6 POTENTIAL DIAGRAM OF A BIPOLAR PROBE

should be defined as that at the top of the space-potential plateau.

There is presumably only a small potential drop between plateau top and sheath edge. Therefore V_1 and V_2, being defined as numerically negative, may be thought of as approximating reasonably well the potentials of the respective collectors relative to zero potential at the top of the plateau. However, rigorously, V_1 and V_2 describe, negatively, the potential differences between collectors and sheath edge. Eq. (27) is a relation only between the potential drop V_1 across the sheath, the positive-ion temperature T_p, negative-ion temperature T_n, electron temperature T_e at the sheath boundary, and the random ion and electron currents, I_p, I_n, and I_e. Eq. (28) shows, in addition to these variables a dependence on sheath radius. Each equation consists of a positive-ion current added to an electron and negative-ion current that is due to the electrons and negative ions that succeed in penetrating the retarding field in the sheath.

One consequence of the difference between the potential of the "plateau" and that of the sheath edge is that the average energy or temperature of the positive ions will be somewhat higher at the sheath edge than

in the undisturbed gas. We shall see, however, that if the ionosphere is initially at temperature equilibrium this increase is only about five per cent under sheath-area-limited conditions and considerably less if the current is limited by orbital motion.

Since the combination of two collectors in space constitutes an isolated system, there can be no net flow of current; hence,

$$i_{T_1} + i_{T_2} = 0 \tag{31}$$

It is reasonable to assume as a very good first approximation that the potential at the outer edge of the sheath is the same for collector No. 1 as for collector No. 2. This justifies stating the relation

$$\delta V = V_1 - V_2 \tag{32}$$

where δV is the voltage applied between the two collectors.

From Eqs. (27) to (32) it is possible to obtain, in principle at least, V_1 and V_2 as functions of δV and the constants of the ionized gas. This determines the manner in which the potential drop across the sheath must vary as the applied voltage δV is changed. Hence, replacing V_1 or V_2 by the equivalent expression in terms of δV provides the desired relationship between i_{T_1} and δV, or between i_{T_2} and δV. This represents the experimentally observable volt-ampere curve for the bipolar probe.

In view of the complicated manner in which the potentials V_1 and V_2 appear in Eqs. (27) and (28), for cylindrical probes, the exact dependence of V_1 or V_2 on δV would be very difficult to find, except by

graphical methods. Fig. 7 shows how a graph of the bipolar characteristic $i_T = f(\delta V)$ can be obtained from the two single-probe plots $i_{T_1} = f(V_1)$ and $i_{T_2} = f(V_2)$. The latter plot is inverted so that the condition $i_{T_1} = -i_{T_2}$ is satisfied by any pair of intersections of the curves with

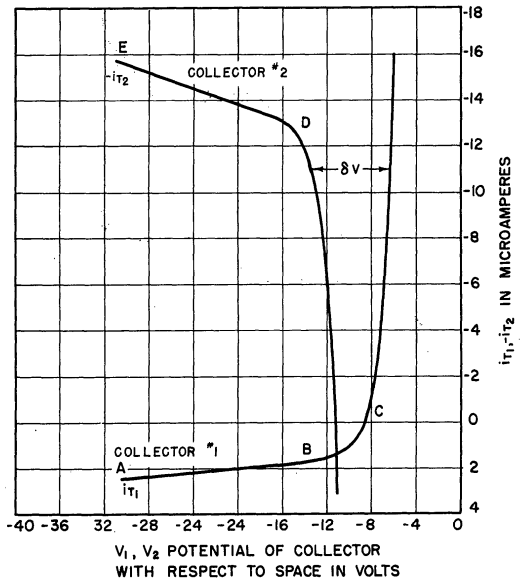

FIG. 7
THE SINGLE-PROBE VOLT-AMPERE CURVES OF
A BIPOLAR PROBE

a horizontal line. For each value of the current the distance between these intersections is the corresponding value of δV. The resulting curve is shown in Fig. 8.

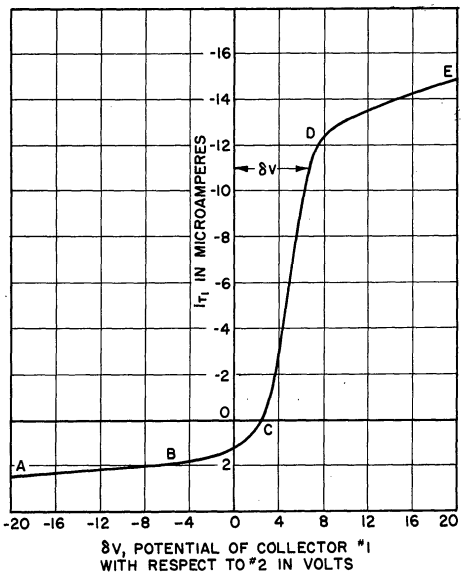

FIG. 8
THE VOLT-AMPERE CURVE OF A BIPOLAR PROBE

The computation of the characteristics of an ionized gas from such curves for a bipolar probe is facilitated by the fact that some parts of the bipolar-probe curve have very nearly the same shape as a single-probe curve. For large negative values of V_1, the electron current to the large collector rises so steeply that V_2 can be considered constant. Except for the different location of the origin, the portion A-B of the bipolar-probe and single-probe curves are then identical. This will apply also to the part B-C if the ratio of the probe areas A_1/A_2 is very small. If this ratio is not too small, V_1 may be considered constant for large positive values of δV, so that the part D-E of the bipolar curve (Fig.8) will be equal to the corresponding part of the curve $-i_{T_2} = f(V_2)$. The conditions to be satisfied in the two cases, respectively, are

$$A_1/A_2 \exp\left[eV/kT_e\right] \ll 1 \tag{33}$$

$$A_1/A_2 \exp\left[eV/kT_e\right] \gg 1 \tag{34}$$

It is possible therefore to use the various methods for computation of the characteristics of an ionized gas from experimental data that were presented in connection with the single probe, if the probe is so designed that the above criteria are satisfied at the appropriate points of the bipolar volt-ampere curves. The part A-B of the curve supplies data for a plot of $(i_p)^2$ vs. δV for computation of the ion density from Eq. (19). The intercept of this line on the horizontal axis represents $V_2 + T_p/11{,}600$ and thus roughly calibrates δV in terms of the gas potential if the current to the probe is known to be limited by orbital motion.

If the criterion for sheath-area-limited ion current to collector No. 2, as well as Eq. (34), are satisfied, the method involving Eq. (25)

can be used to compute $N_p\sqrt{T_p}$. If N_p has been determined from the small-probe characteristic, T_p can thus be obtained. It should be remembered that these values of N_p and T_p represent the conditions at the sheath edge, not in an undisturbed region of the gas. If different points on the curve are used for computation, different values of T_p and N_p may result, since sheath thickness and across-the-sheath potential difference will vary with δV.

If the negative-ion and electron temperatures are equal, a plot of Eq. (26) will give this temperature from the slope of the line. As mentioned above, it is not practical to calculate the electron concentration, or rather the sum of negative-ion and electron concentrations weighted inversely as the square root of their masses, from the negative-particle current obtained from the part B-C of the probe curve by subtraction of the extrapolated positive-ion current. On the other hand, if these concentrations were known, the space potential could be much more accurately obtained by this method than by extrapolation of the $(i_p)^2$ vs. δV line.

Johnson and Malter[17] have used some convenient procedures to obtain the electron temperature of a positive-ion-electron plasma from the bipolar-probe curve under circumstances when the condition (33) is not satisfied. These methods are not reviewed here because they are not easily adaptable to the probe geometry used so far, nor to the one suggested for future rocket measurements.

C. The Region of Ambipolar Diffusion

One of the most difficult problems in evaluation of rocket probe data, even if obtained by a probe of considerably improved design, is the

calculation of the difference in charged-particle concentrations and temperatures between the undisturbed ionosphere and the sheath edge. It is a problem of ion mobility or diffusion, for which no precise theory in satisfactory agreement with observations exists. The only alternative to the application of an adequate theory is laboratory experiments so arranged that they can be extrapolated to the actual probe conditions with strict adherence to the laws of similitude. The nature of the ionosphere as an electrodeless discharge with pure volume recombination makes such experiments very difficult. However, a detailed discussion of this question is beyond the scope of the present report.

We shall here discuss the variations of charged-particle concentrations and temperature from the point of view of an approximate theory.[13,14] The basic assumptions in this approach are:

1. The flow is completely viscous in the ambipolar diffusion region; this region borders directly on the sheath, where the viscosity is negligible, certainly a considerable oversimplification of the actual conditions.
2. A steady state exists.
3. $N_p = N_n + N_e$, and the ratios between these concentrations are constant.
4. $N_n = N_{n_o} \exp(eV/kT_n)$ (retarding field, V negative) (35)
5. $N_e = N_{e_o}/\exp(eV/kT_e)$ (36)

The positive-ion current depends on the positive-ion concentration gradient, the positive-ion temperature gradient, and the potential gradient according to the equation

$$I_p = eN_p \cdot D_p \left\{ \frac{1}{N_p} \text{ grad } N_p + \frac{1}{V_p} (\text{grad } V_p + \text{grad } V) \right\} \qquad (37)$$

where D_p is the diffusion coefficient of the positive ions and V_p is the voltage equivalent of the positive-ion temperature.

Continuity requires that at every point the divergence of this current be equal to the difference between the ionization rate and the recombination rate. The ionization rate is independent of the ion and electron concentrations while the recombination rate can be considered to vary with the square of the positive-ion concentration.

$$\frac{1}{e} \text{ div } I_p = -\alpha (N_{po}^2 - N_p^2), \qquad (38)$$

where N_{po} is the positive-ion concentration in the undisturbed plasma.

It is thus evident that the ambipolar diffusion in the ionosphere is quite different from the diffusion in a gas-discharge tube, the main reasons being the absence of sustaining electrodes and different predominant processes of ionization and recombination.

To get a first approximate solution it is convenient to assume temperature equilibrium: $T_p = T_n = T_e$ = the gas temperature. Then, according to the assumptions 3 to 5 we can write

$$\text{grad } V = \frac{kT_e}{e(N_n + N_e)} \text{ grad } (N_n + N_e) \qquad (39)$$

$$I_p \approx eD_p \left[1 + (T_e/T_p) \right] \text{grad } N_p \approx 2eD_p \text{ grad } N_p \qquad (40)$$

$$\nabla^2 N_p \approx -\frac{\alpha}{2D_p} (N_{po}^2 - N_p^2) \qquad (41)$$

Since the ambipolar-diffusion region is known to be very large compared to the collector dimensions a spherical geometry with $\partial/\partial\phi = \partial/\partial\theta = 0$ will approach the actual conditions over a very large fraction of the region.

Introducing the new variable

$$\Phi = r(N_{p_o} - N_p) \tag{42}$$

we obtain

$$\frac{\partial^2\Phi}{\partial r^2} = + \frac{\alpha}{2D_p}(N_{p_o} + N_p) \cdot \Phi \tag{43}$$

An approximate solution good for very small variations of N_p results if $N_{p_o} + N_p$ is replaced by $2\,N_{p_o}$

$$N_p = N_{p_o} - \frac{Q}{r}\, e^{-\beta r} \tag{44}$$

where N_{p_o} and Q are constants to be determined from the boundary conditions at the sheath edge and

$$\beta = \sqrt{\frac{\alpha\, N_{p_o}}{D_p}} \tag{45}$$

If numerical values of the order of magnitude encountered in this experiment are introduced in Eq.(44), it will be found that the variations of N_p with r are not always small, so that the linear approximation to Eq.(41) may be questionable. Since the solution is continuous and monotonic within the range r = a to r = ∞, suitable limits for its variation can be easily established:

$$2\,\alpha r\, N_a\,(N_{p_o} - N_p) \leq -\frac{\partial^2}{\partial r^2}(rN_p) \leq 2\,\alpha r\, N_{p_o}\,(N_{p_o} - N_p) \tag{46}$$

$$N_{p_o} - \frac{Q_1}{r} e^{-\beta_1 r} \leq N_p \leq N_{p_o} - \frac{Q_2}{r} e^{-\beta_2 r} \tag{47}$$

where N_{p_o}, Q_1, and Q_2 are constants to be determined from the boundary conditions and where

$$\beta_1 = \sqrt{\frac{\alpha N_a}{D_p}} \tag{48}$$

$$\beta_2 = \sqrt{\frac{\alpha N_{p_o}}{D_p}} \tag{49}$$

N_a is the positive-ion concentration at the sheath edge (r = a).

The recombination coefficient α has been estimated to 10^{-8} cm^3/sec or 10^{-14} m^3/sec. The diffusion coefficient is approximately

$$D_p = \frac{16\ e\ V_p}{9\pi\ m_g} \cdot \ell_p \tag{50}$$

where m_g is the mass of a gas molecule and ℓ_p the mean free path of the ions. For an ion density as high as 10^{12} ions/m^3, β is approximately 0.022.

In the part of the diffusion region that is of particular interest βr is so small that the difference between the two limits in Eq. (47) is insignificant.

For very small sheath dimensions a cylindrical solution of the diffusion problem may be of interest. Linearizing Eq. (41), as before, we obtain the following solution

$$N = N_{p_o} - Q\ H_o\ (j\beta r) \tag{51}$$

where H_o is the Hankel function of order zero and β has the same meaning as in the spherical solution.

In order to determine the relation between the positive-ion concentration in the undisturbed ionosphere and that at the sheath edge, we make use of the continuity of the ion-current density at the sheath edge.

The spherical solution gives

$$\frac{i_n \cdot 4\pi r^2 \cdot I}{4\pi a^2} = \frac{i_n I}{\gamma^2} = e D_p \left(1 + \frac{V_e}{V_p}\right) \text{ grad } N_p$$

$$= e D_p \left(1 - \frac{V_e}{V_p}\right) (N_{po} - N_a)\, a \left(\frac{1}{a^2} + \frac{\beta}{a}\right) \qquad (52)$$

where V_e is the voltage equivalent of the electron temperature.

After introduction of Eqs. (7) and (50) we obtain

$$\frac{N_{p_o} - N_a}{N_a} = \frac{3}{4\sqrt{2}} \cdot \frac{a}{\ell_p} \cdot \frac{1}{\left(1 + \frac{V_e}{V_p}\right)(1 + \beta a)} \cdot \frac{i_n}{\gamma^2} \cdot \qquad (53)$$

When βa is small, $V_e = V_p$, and the current through the sheath is limited by sheath area, this reduces to

$$\frac{N_{p_o} - N_a}{N_a} = .265 \cdot \frac{a}{\ell_p} \qquad (54)$$

When the current is limited by orbital motion i_n is independent of γ so that the left member of (53) is inversely proportional to the sheath radius instead of directly proportional as in (54). A maximum must occur between these two extremes, probably in the neighborhood of the transition from sheath-area-limited current to orbital-motion-limited current.

For very large sheath radius ($\beta a \gg 1$) Eq. (54) becomes

$$\frac{N_{p_o} - N_a}{N_a} \approx \frac{0.265}{\beta \ell_p} \qquad (55)$$

Under ideal cylindrical conditions the corresponding relations to Eqs. (52) and (53) are

$$\frac{i_n \cdot 2\pi r \boldsymbol{\ell} \cdot I}{2\pi a \cdot \boldsymbol{\ell}} = \frac{i_n \cdot I}{\boldsymbol{\gamma}} = e D_p \left(1 + \frac{V_e}{V_p}\right) Q \, j \beta H_1(j\beta a) \qquad (56)$$

$$\frac{N_{p_o} - N_a}{N_a} = \frac{3}{4\sqrt{2}} \cdot \frac{a}{\boldsymbol{\ell}_p} \left(1 + \frac{V_e}{V_p}\right) \frac{H_o(j\beta a)}{j\beta a \, H_1(j\beta a)} \frac{i_n}{\boldsymbol{\gamma}} \cdot \qquad (57)$$

Here

$$\frac{H_o(j\beta a)}{j\beta a \, H_1(j\beta a)} \approx \log \frac{2}{1.781 \, \beta a} \quad \text{for } \beta a \ll 1 \qquad (58)$$

$$\approx \frac{1}{\beta a} \quad \text{for } \beta a \gg 1 \qquad (59)$$

For sheath-area—limited current, $V_e = V_p$, and $\beta a \ll 1$ we now get, in analogy with Eq. (54),

$$\frac{N_{p_o} - N_a}{N_a} \approx 0.265 \cdot \log \frac{2}{1.781 \, \beta a} \cdot \frac{a}{\boldsymbol{\ell}_p} \cdot \qquad (60)$$

For $0.02 \leq \beta a \leq 1.0$ the fraction to the left in Eqs. (58) and (59) lies between the corresponding limits of 4.02 and 0.70. The drop in ion concentration is consequently appreciably larger in an ambipolar diffusion region of cylindrical shape than in one of spherical shape of the same radius.

The two limits obtained by using $\beta = \beta_1$ and $\beta = \beta_2$, Eqs. (53) and (54), may in the cylindrical case differ appreciably even in the neighborhood

of the sheath edge and for small values of βa. It may therefore become desirable to have a complete solution of the nonlinear equation (41) in the form of a numerical table or a graphical map.

The assumption of a constant positive-ion temperature throughout the diffusion region introduces an error whose order of magnitude can easily be checked after the approximate numerical solution of the diffusion problem has been found according to the procedure outlined above. The potential gradient at the sheath edge is obtained from Eq. (39), and the voltage equivalent of the positive-ion temperature

$$V_p = \frac{V_g}{2} \pm \sqrt{\frac{V_g^2}{4} + \sqrt{\frac{2}{3}}\ (\boldsymbol{\ell}_p \text{ grad } V)^2} \qquad (61)$$

The product $\boldsymbol{\ell}_p$ grad V can be calculated from Eqs. (39) and (40) since the ambipolar diffusion region is very nearly neutral, so that $N_p \approx N_e + N_n$. For a spherical sheath,

$$\boldsymbol{\ell}_p \cdot \text{grad } V \approx V_e \frac{i_n}{r^2} \cdot \frac{3}{4\sqrt{2}\left(1 + \frac{V_e}{V_p}\right)} \approx .265\ V_e \qquad (62)$$

for sheath-area-limited current and less for orbital-motion-limited current. If the electron temperature is equal to the gas temperature, this means according to Eq. (62) that the ion temperature exceeds the gas temperature by three per cent or less. Assumption of a cylindrical sheath leads in this case to the same result. As long as the negative-particle temperature is approximately equal to the gas temperature, the increase in positive-ion temperature in the diffusion region is insignificant.

The methods for calculation of positive-ion density that were given in the preceding sections assumed an ion density at the sheath edge independent of the collector potential. In a cylindrical geometry this condition is not satisfied even if the collector radius is very small (Eq. 60), and the slope of the various plots used will not be so simply related to the positive-ion density at the sheath edge as indicated by Eqs. (18) and (27). However, if the space potential can be determined from other data, such as the negative-particle current, and the current is known to be limited by orbital motion, the sheath-edge positive-ion concentration can be calculated for every point on the probe characteristic. The drop in the diffusion region can then be obtained from Eq. (57).

When the current is limited by sheath area Eq. (27) in our procedure is invalidated because

$$\frac{d(\log i)}{d(\log V)} \neq \frac{d(\log i_n)}{d(\log \eta)} \tag{63}$$

Instead we have

$$i = i_n \cdot N_a \cdot A \tag{64}$$

$$\frac{d(\log i_n)}{d(\log \eta)} = \frac{\dfrac{d(\log i)}{d(\log V)}}{1 - \dfrac{d(\log N_a)}{d(\log i_n)}} \tag{65}$$

Since $i_n = \gamma$ we can find

$$\frac{d(\log N_a)}{d(\log i_n)} = \frac{d(\log N_a)}{d(\log \gamma)} = \frac{d(\log N_a)}{d(\log a)} = \frac{a}{N_a}\frac{dN_a}{da} \tag{66}$$

from Eq. (57). Since the two unknown variables N_a and γ are related to the observed quantities i and V by transcendental equations, numerical or graphical solutions have to be used. A zero-order approximation of N_a may be obtained from Eq. (27) and Fig. 4 by considering N_a independent of a, and first and higher-order approximations by using the lower-order N_a and γ in Eqs. (57), (66), (65), and (27).

GENERAL DISCUSSION OF THE IONOSPHERE PROBE

The application of the bipolar probe to the determination of the characteristics of the E-layer of the ionosphere will be discussed in general terms in this section. After presentation of some preliminary experimental results a number of sources of error and design precautions to minimize these will be considered in the next section.

The first consideration is choice of geometry. Analytical solutions of reasonably modest complexity exist only for three typical geometries: plane, circularly cylindrical, and spherical. The choice of a cylindrical arrangement has been anticipated in the preceding presentation, for rather obvious reasons: It is structurally adaptable to mounting on a rocket, and it has proved its worth during many years of application to gas-discharge tubes, primarily as single probes but to a lesser extent also as bipolar probes.[15] The structural difficulty connected with the cylindrical probe is the demand that it be long, not only compared to its diameter, but compared to the sheath diameter. This demand can be somewhat relaxed, if guard electrodes are used, maintained at the same potential as the collectors and protecting the latter from most of the currents caused by the non-cylindrical field at the ends. For any measurements of more than order-of-magnitude accuracy with a structure of practical dimensions, such guard electrodes are mandatory. When guard electrodes are used $i_{T_1} \neq -i_{T_2}$, and two currents have to be measured rather than one (Fig. 9). The procedure for reduction of data will be the same as described above, however, since single-probe approximations were used throughout. Dr. Eric Beth has brought to the authors' attention a suggestion to elaborate the guard-electrode system

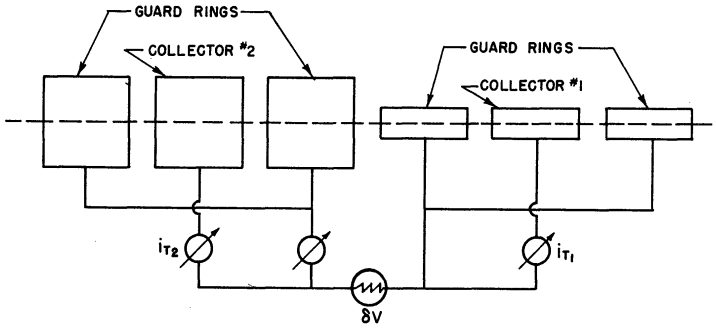

FIG. 9
BIPOLAR-PROBE SYSTEM WITH GUARD ELECTRODES

by subdividing the collectors further and measuring the current collection of each individual section; the approximation to proportionality between current collected and axial length would show how closely the sheath geometry approached a cylindrical one. Whether or not such an elaborate arrangement can be used on future flights will probably be determined by practical considerations, such as available telemetering channel space.

The second problem in collector design concerns the choice of collector diameters. According to the single-probe theory discussed in a preceding section a combination of a sheath-area-limited collector and an orbital-motion-limited collector would have the merit of giving explicit information of both positive-ion density and positive-ion temperature. In order to apply this design criterion we determine from Fig. 3 the transition point between sheath-area-limited current and orbital-motion-limited current:

$$\frac{T_p}{N_p r^2} = 0.7 \times 10^{-4}. \qquad (67)$$

Thus, if the maximum value of N_p is 10^{12} per cubic meter and T_p = 300°K, the radius of the collector must be smaller than 2 mm in order to give orbital-motion-limited current. The design of such a probe for mounting on a rocket with appropriate guard electrodes meets with structural problems; also, the current collected will be so small that errors due to leakage, drift, etc., may become appreciable. However, these difficulties may not be insurmountable.

These design considerations appear in a somewhat different light when the ambipolar diffusion is taken into account. An accurate knowledge of the positive-ion concentration at the sheath edge is of no particular value unless the drop in concentration from ambipolar diffusion can be determined with comparable accuracy. This drop is negligible in a spherical geometry if the sheath radius is small compared to four times the mean free path of the ions at the transition point between the orbital-motion-limited and the sheath-area-limited current (Eqs.53 and 54). The criterion in a spherical geometry corresponding to the cylindrical-geometry criterion given in Eq.(67) has not yet been worked out by the authors, but most likely the radius of the spherical probe will be larger but of the same general order of magnitude as that of a cylindrical probe, say 5 to 10 mm. The practical difficulties connected with such a probe will be even larger than in the case of the cylindrical probe.

The ambipolar diffusion furnishes an additional reason for designing a cylindrical probe for orbital-motion-limited current, because then the ion-density calculation breaks down into two independent operations, one for the sheath and one for the diffusion region, while a sheath-area-limited probe gives simultaneous transcendental equations that have

to be solved by successive approximations. Since the design of a probe that has orbital-motion-limited current at all altitudes appears to meet practical difficulties, an additional collector whose current is always limited by sheath area will be helpful to bridge the transition region of the small probe. At this point it becomes evident that the plan to determine the ion temperature from the data of two collectors should be abandoned, since the introduction of another variable in the diffusion problem makes the computation hopelessly complicated. Since it appears that the approximate temperature equilibrium in the ionosphere is or can be established from other experimental data, this is not a very important sacrifice. Actually the negative-particle-energy distribution indicated by the part B-C of the probe curves (Figs. 7 and 8) may prove that such an equilibrium prevails; it is difficult to imagine circumstances under which the positive ions have substantially higher energies than the electrons.

The diffusion theory is only approximate; consequently experimental verification is required on several points before any ion concentrations calculated from bipolar-probe measurements can be accepted with confidence in their accuracy. The diffusion coefficient (Eq. 50) and the mean free path of the positive ions at 250-300°K should be measured in the laboratory under conditions resembling those in the ionosphere as closely as possible. Knowledge of the volume recombination coefficient is also required in the cylindrical diffusion problem but not in the spherical one; it is at least roughly known from radio-propagation measurements.

PRELIMINARY EXPERIMENTAL RESULTS

A. Flight Data and Equipment

The previous presentation has been based on a number of idealizations and assumptions that can be reliably justified or improved only by careful comparison of experimental observations and theoretical predictions or, possibly, by an interpretation of data in terms of a revised set of assumptions.

There have been three V-2 rockets on which probes were carried. The main purpose of the participation of the University of Michigan in these flights was to measure pressure and temperature in the upper atmosphere, so that the probe was to some extent in the position of a stepchild. Considerations of space and weight made it necessary to use a rather crude probe configuration, so that accurate determination of the E-layer characteristics was out of the question. The main purpose of including the probe was to prove that the scheme was workable and to gain experience in the various instrumentation problems connected with it. It was hoped that an attempt to reduce the data would show them to be compatible with results obtained from radio-propagation measurements and give valuable hints about secondary phenomena, sources of error, etc. These hopes have been completely justified.

Of the three V-2 firings, November, 1946, February, 1947, and December, 1947, only the last one provided data that could be considered suitable for analysis. Instrumentation difficulties and rocket spin made the data from the earlier two flights nearly completely worthless. The following will therefore concern the December 1947 flight only. Fig. 10 shows the nose piece of the rocket carrying five ionization guages and a

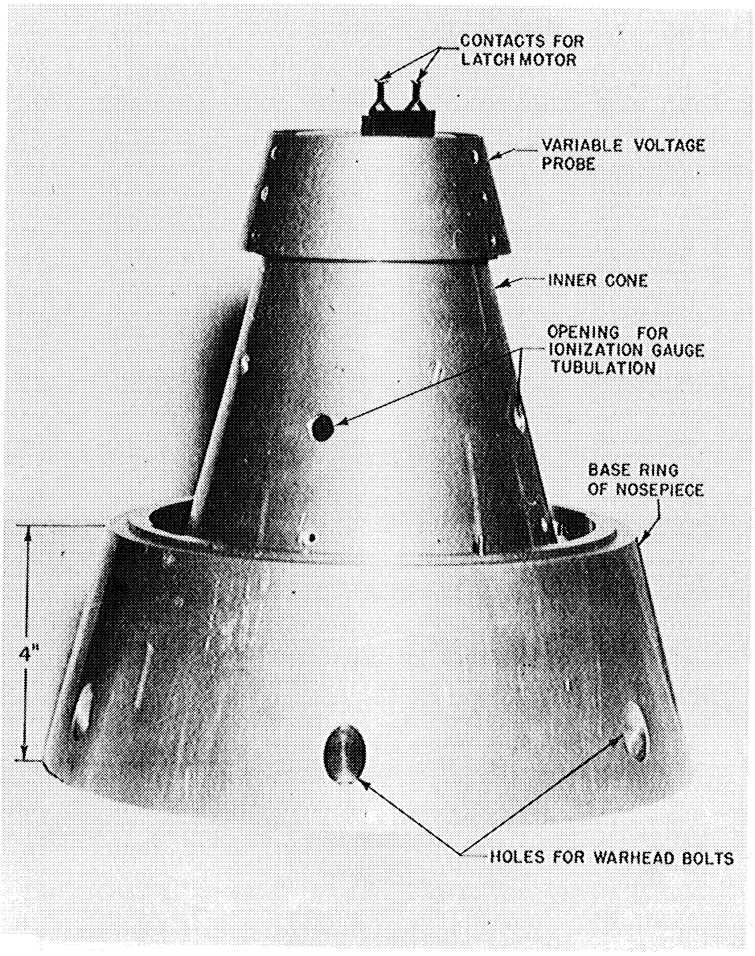

FIG. 10
NOSEPIECE WITH OUTER CONE SURFACES REMOVED

probe. To reduce drag and protect the gauges at low altitudes, the nose piece was covered by a smooth cone, which was split and thrown off at an altitude of 45 km. The probe (collector No. 1) was a ring in the shape of a truncated cone mounted on insulators at the top of the nose piece. The requirements imposed by the pressure measurements left room only for this very short probe which does not by far approach the long cylinder desirable for the purpose of reducing the data by means of formulas derived for an ideally cylindrical geometry. The approximate dimensions can be seen from the scale at the bottom of the figure. The scanning saw-tooth-voltage generator had a period of 0.6 second and an amplitude of $\pm$ 20 volts.

This voltage was applied between the probe and the nose piece (collector No. 2). A sensitive electronic measuring circuit was used to record the current flow between the collectors. The instantaneous value of this current was transmitted to a recording oscillograph on the ground by means of a radio telemetering system.

The resulting current-versus-voltage oscillogram was transformed into a set of volt-ampere curves, representative samples of which are shown in Figs. 11-14. The saw-tooth voltage was not continuously measured but was assumed to vary linearly with time within each cycle and to maintain its amplitude constant. Experiments have confirmed the linearity within 10 per cent in the range ± 15 volts. The trajectory of the rocket

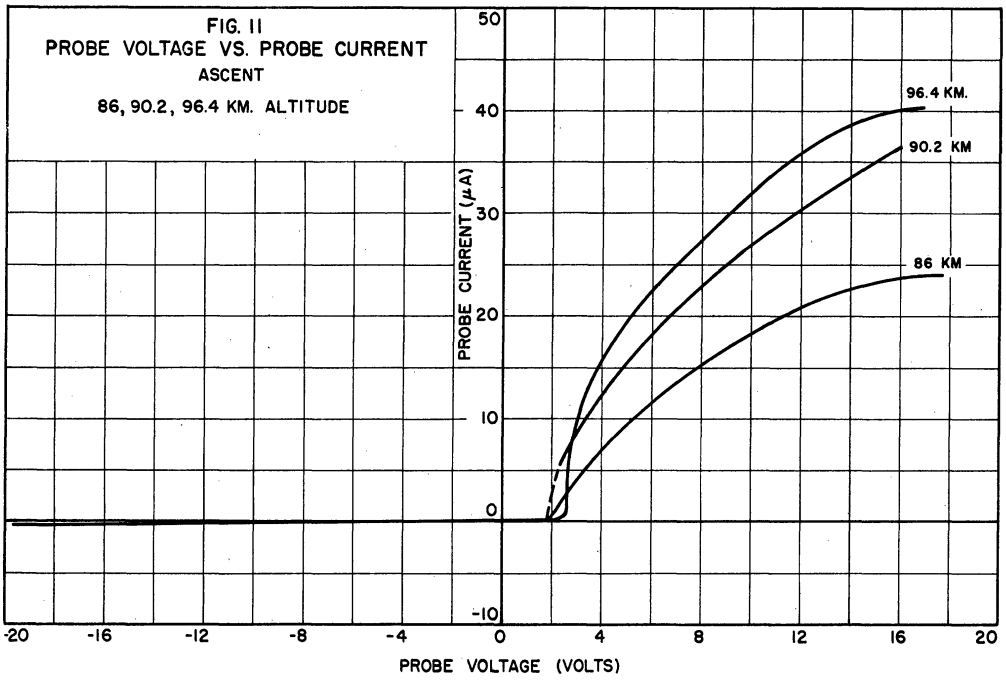

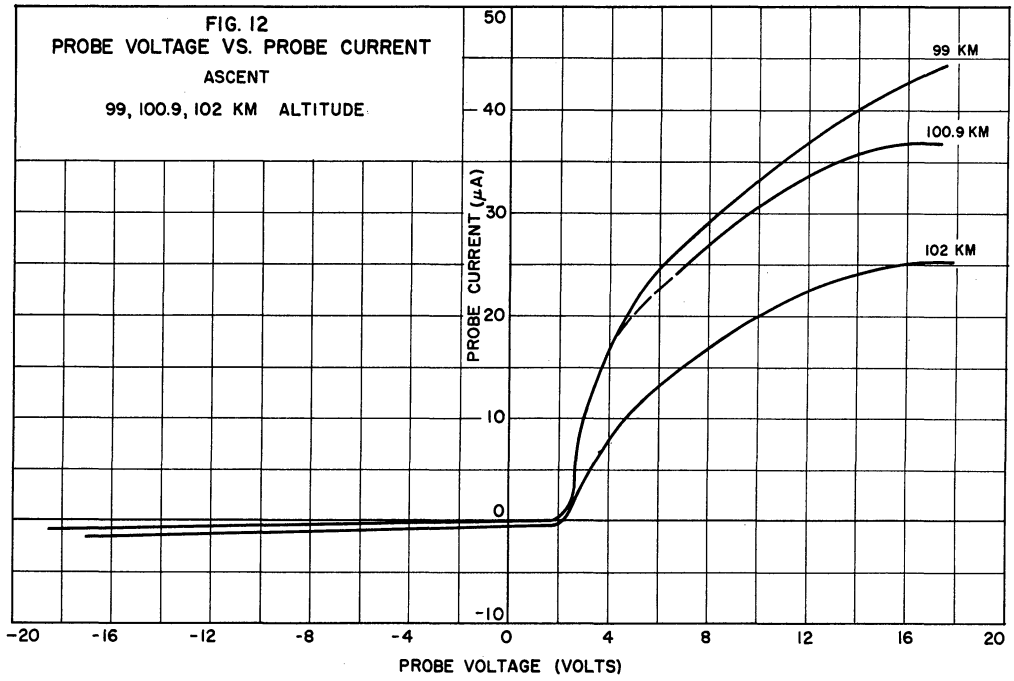
FIG. 12
PROBE VOLTAGE VS. PROBE CURRENT
ASCENT
99, 100.9, 102 KM ALTITUDE
99 KM
100.9 KM
102 KM
PROBE CURRENT (μA)
50
40
30
20
10
0
-10
-20
-16
-12
-8
-4
0
4
8
12
16
20
PROBE VOLTAGE (VOLTS)

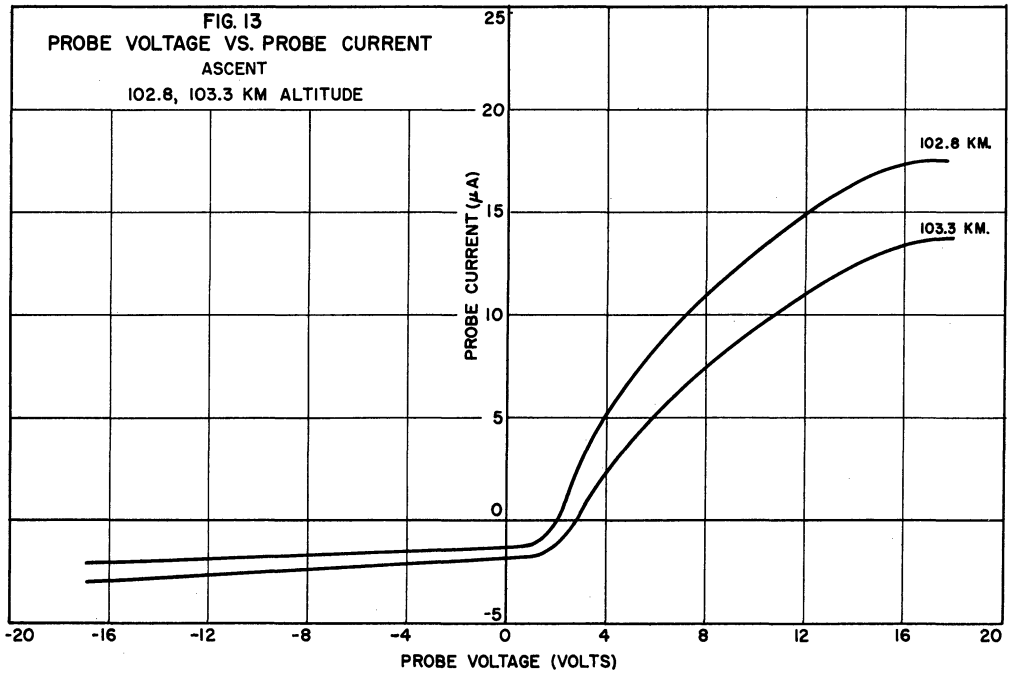
FIG. 13
PROBE VOLTAGE VS. PROBE CURRENT
ASCENT
102.8, 103.3 KM ALTITUDE
102.8 KM.
103.3 KM.
PROBE CURRENT (μA)
25
20
15
10
5
0
-5
-20
-16
-12
-8
-4
0
4
8
12
16
20
PROBE VOLTAGE (VOLTS)

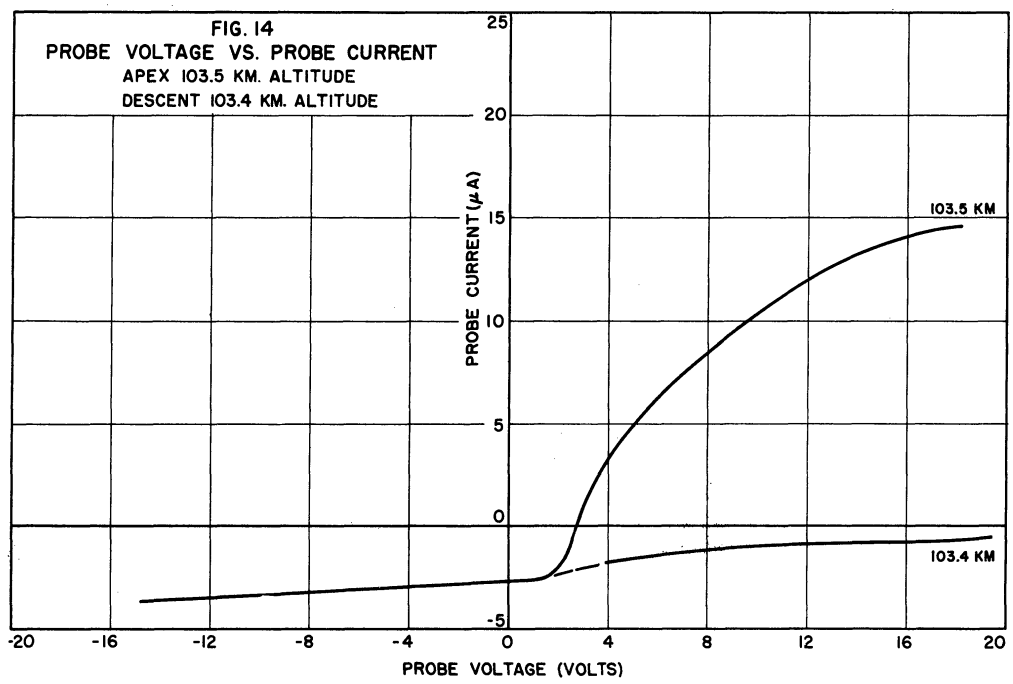

was recorded simultaneously from a radar station, so that the correct altitude could be associated with each volt-ampere curve. The radar data from the December 1947 flight are shown in Fig. 15. This is a plot of the radar trajectory with the time elapsed since the firing indicated every 10 seconds on the curve. Information concerning rocket aspect, total velocity, mean free path, and air density is also shown. It can be seen that the rocket attained a maximum altitude of only 103.5 km, which is appreciably below that anticipated for the probe measurements. The telemetering record shows that the probe current remained too small to be measured until an altitude of about 70 km was reached. From there on, readable currents were observed for the positive swing of the probe voltage (i.e., voltage on collector No. 1) during each scan. This is an indication of measurable positive-ion collection by collector No. 2 (the rocket itself) above 70 km. It was not until an altitude of about 98 km was reached that

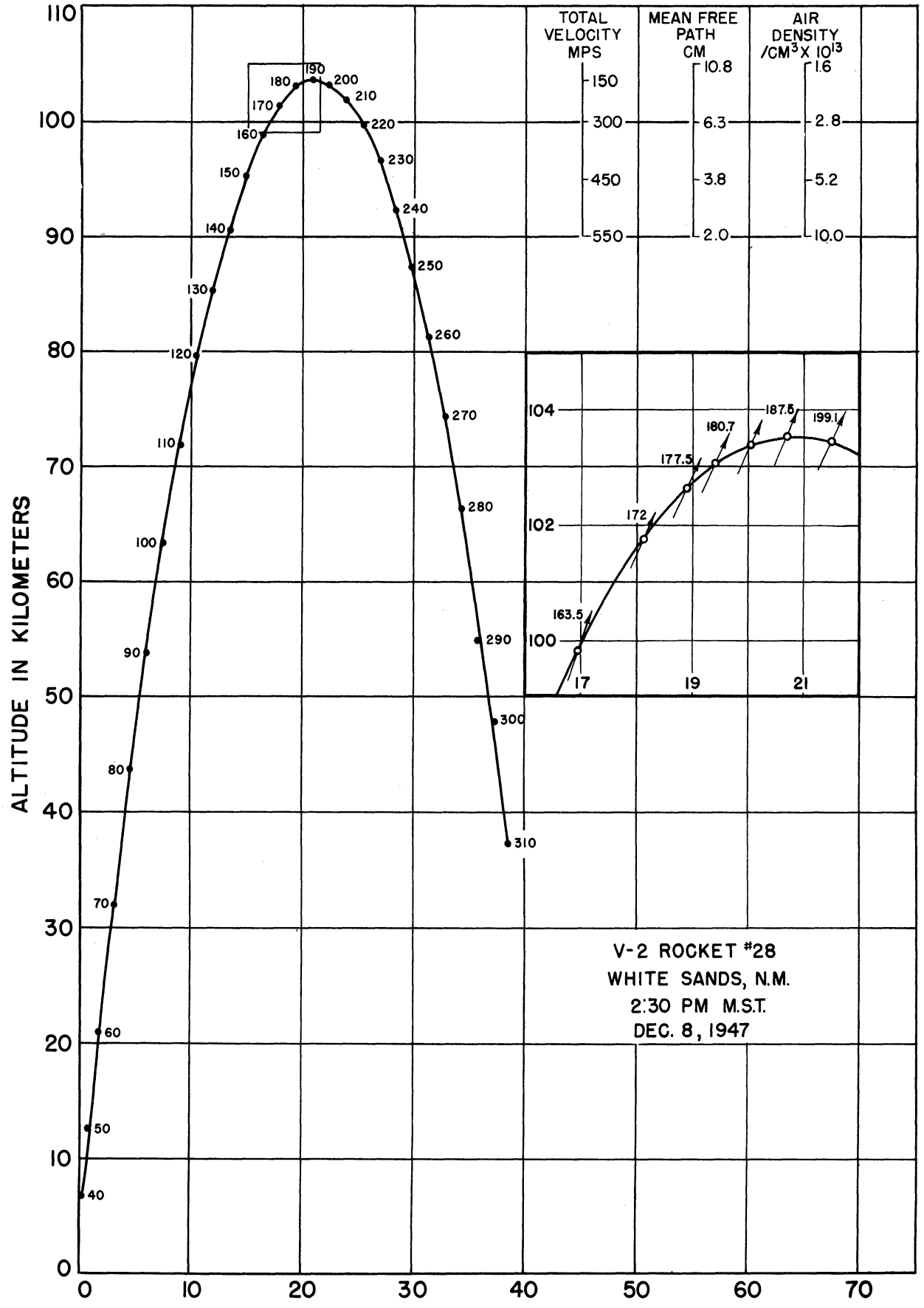

FIG. 15
DATA OF THE FLIGHT DEC. 8, 1947

reasonably accurately readable currents were observed during the negative swing of the probe voltage. This indicates that at this altitude the positive-ion collection to the probe or small collector became measurable. Of course, the surface area of No. 2 collector was very much greater than that of the small No. 1 collector. As the rocket passed the crest the data show quite unexpected variations, the outstanding effect being that the positive-swing current dropped to zero. At passage of the rocket over the crest two of the five pressure gauges mounted adjacent to the probe (see Fig. 9) indicated a rapid drop in air density, which shows that the air about the nose piece was violently disturbed by the presence of the rocket. Under such conditions the collector current is difficult to predict, and the subsequent data are useless for determination of the constants of the ionosphere. The range of utilizable data is indicated by the rectangular inset in Fig. 10; the enlarged inset shows the range for which experimental volt-ampere curves were taken as well as the approximate rocket aspect at that time.

It should be stated here that even the data above characterized as "utilizable" must be expected to deviate considerably from the relations developed in the preceding sections. The most obvious reasons for this are the noncylindrical geometry and the overlapping of the electric fields from the two collectors. Other reasons, such as non-Maxwellian velocity distributions of electrons and ions, may exist, however, and more than one interpretation of the data is certainly possible. In an advance publication[17] two of the present authors presented a tentative interpretation in terms of electron and ion temperatures considerably higher than those expected in the undisturbed ionosphere and an electron drift velocity

superposed on the Maxwellian distribution. The main supporting evidence for this interpretation was the difference of potential of about two volts between the collectors at the sharp bend in the probe curve and the slope and curvature of the curves of log i_e vs. δV. (See Appendix III, Fig 37 .) However, the error in the assumed voltage variation along the saw tooth plus contact potentials in the collector circuit may very well amount to two volts. The fact that this difference of potential remains nearly constant while the ion and electron densities vary several orders of magnitude makes an instrumental origin much more probable than an ionospheric one. The variation of the negative-particle current with potential difference, on the other hand, is necessarily strongly influenced by the interaction of the sheaths and diffusion regions of the two collectors; deviations from the ideal theory are consequently not surprising. In short, the evidence supporting an interpretation in considerable disagreement with the prevalent opinion about the characteristics of the E-layer is weak. After careful consideration of the errors and uncertainties involved in the experiment the authors have arrived at a different interpretation which is given below. It is by no means complete, and it leaves many questions unanswered. We still have to revise some of our assumptions of the characteristics of the E-layer in order to bring this interpretation in order-of-magnitude agreement with the electron density data obtained by other methods, but the revisions are less drastic and reportedly supported by other independent evidence.*

Returning to Fig. 15, it is seen that the molecular mean free path varies from about 6 cm to 11 cm within the altitude range of interest.

---

* The authors are indebted to Dr. Eric Beth for information regarding relevant material presented at a seminar at AMC Cambridge Research Laboratories in the summer of 1950.

These figures are based on the pressures simultaneously recorded by the ionization gauges.

It is clear that the geometry of the probe and the sheaths, being far from cylindrical, does not permit more than an order-of-magnitude calculation of E-layer constants. Nonetheless, it may be worthwhile to discuss the edge effects and see if some rough corrections can be made. If we wish to use the cylindrical theory, an "effective length" of the collector, larger than the actual length, has to be used in the computations. The added length should be a function of the sheath thickness or of the difference between the thickness of the probe-sheath and the rocket-sheath thickness.

$$l_{eff} = l + 2\,\gamma\,(a_1 - a_2) \tag{68}$$

where γ is a factor of the order of unity; in the calculations quoted below the value 1.0 has been used.

When the correction becomes large there is very little justification for using the cylindrical theory at all. Since there is a tendency for unipolar fields to become spherical far from their source in terms of the dimensions of this source, the use of the theory of a spherical probe has been considered and some calculations have been made for comparison. The presence of the large collector, the rocket itself, prevents the field from the small probe from assuming spherical shape. Because the latter is located at the extreme tip of the rocket, however, the field may approach spherical shape over a considerable solid angle. The relations for a spherical probe that correspond to Eqs. (17) and (27) are

$$i_n = 1 + \eta \tag{69}$$

$$\frac{d\left[\log (-\alpha)^2\right]}{d(\log \gamma)} = \frac{d(\log \gamma^2)}{d(\log \eta)} = 3 \cdot \frac{i\, dV}{V\, di} - 2 \qquad (70)$$

where $(-\alpha)^2$ is a function of $\gamma = a/r$ analogous to $(-\beta)^2$, also tabulated by Langmuir and Blodgett. A plot of the left member of Eq.(70) as a function of γ is shown in Fig. 16.

Another uncertain element in the reduction of data from the December 1947 flight is the area A_2 of the large collector, that is, the rocket itself. It appears probable that the paint covering the main body of the rocket was a sufficiently good insulator to reduce the effective area to that of the nose piece. Because of the uncertainty this introduces no use can be made of the data obtained for large positive values of the saw-tooth voltage.

The evaluation of the preliminary data obtained from the December, 1947, flight involves two essential operations: calculation of the E-layer characteristics from the data, and a check whether or not the data as a whole are in agreement with theory. If not, reasonable explanations of the deviations should be found. The latter of the two operations can in this case only be qualitative, but it is nonetheless essential in order to establish confidence in the bipolar-probe method as a tool for exploration of the ionosphere.

The two operations are so closely related that they cannot be treated separately. The presentation of the results will, therefore, be accompanied by the discussion of the expected or unexpected character of the data as their relationships suggest.

B. Negative Probe Current and Positive-Ion Density

In order to get an order-of-magnitude estimate of the ion density in the E-layer from the data collected on the December, 1947, flight, the

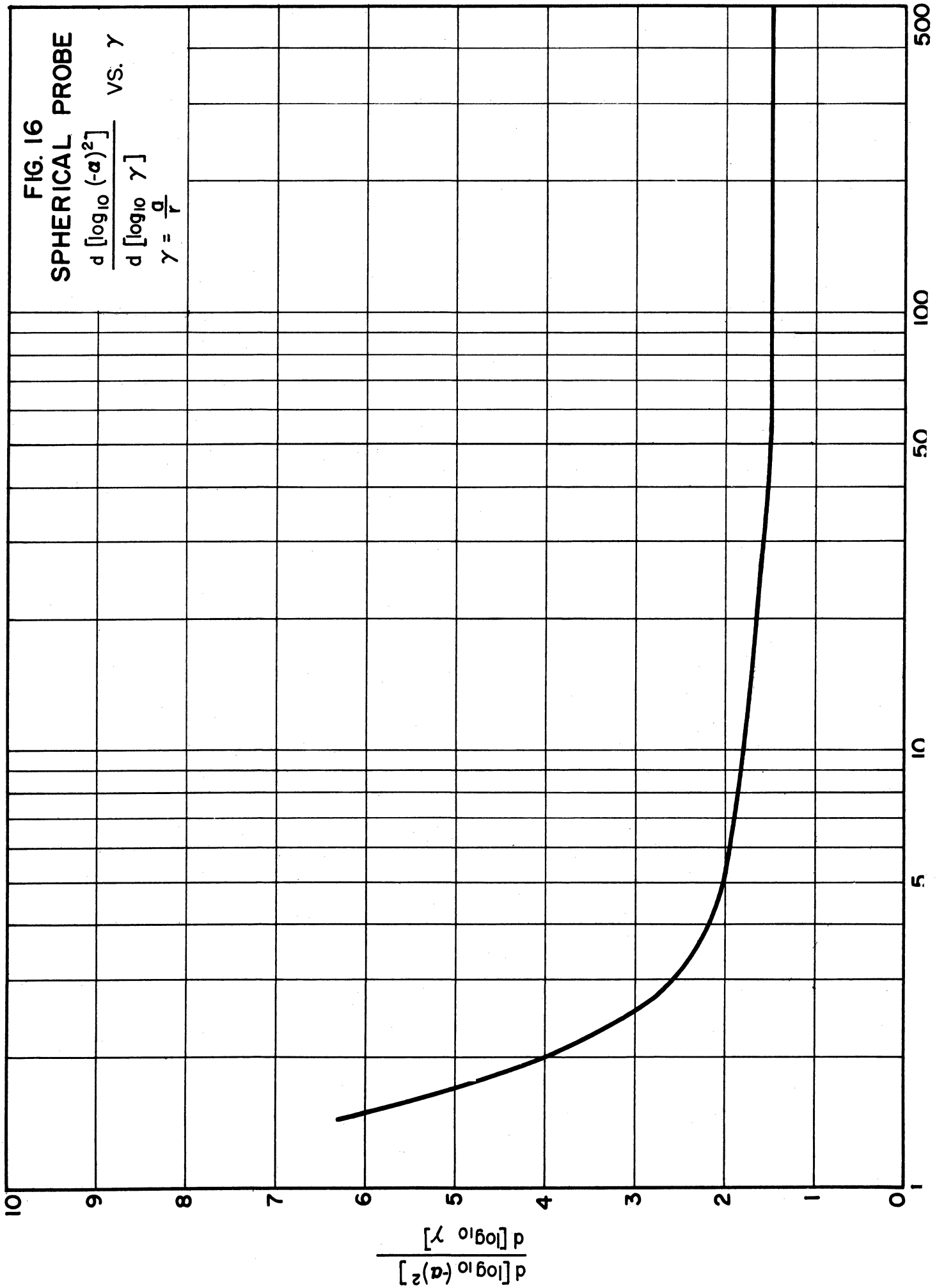
FIG. 16
SPHERICAL PROBE
$\frac{d\,[\log_{10}(-a)^2]}{d\,[\log_{10}\gamma]}$ VS. γ
$\gamma = \frac{a}{r}$
$\frac{d\,[\log_{10}(-a)^2]}{d\,[\log_{10}\gamma]}$
0
1
2
3
4
5
6
7
8
9
10
1
5
10
50
100
500

previously reviewed methods of computation have been used under different sets of idealized assumed conditions. The results will be presented and discussed in this section. The areas of the data will be selected where one or the other of the sets of assumptions leads to the best approximation.

The alternative conditions covered by the computations are as follows:

a) Cylindrical geometry, effective length of probe according to Eq.(40) (γ = 1), current limited by sheath area, ion temperature 300°K

b) Same as condition a), except for a positive-ion temperature of 3000°K

c) Cylindrical geometry, effective length of probe arbitrarily assumed to be 13 cm, current limited by orbital motion.

d) Spherical geometry, current limited by sheath area, ion temperature 300°K

e) Same as condition d), except for an ion temperature of 3000°K

f) Spherical geometry, current limited by orbital motion, ion temperature 300°K

The data utilized at each altitude are the coordinates and slope of the probe characteristics at δV = -10 volts. The probe potential, however, must be referred to space potential rather than rocket potential. If we assume that the electron temperature is only a few hundred degrees Kelvin, the space potential will differ only by a few tenths of a volt from the probe potential for which the sharp upward bend in the curve occurs. At δV = -10 volts the actual probe potential is then roughly -12 volts. The results are plotted in Fig. 17.

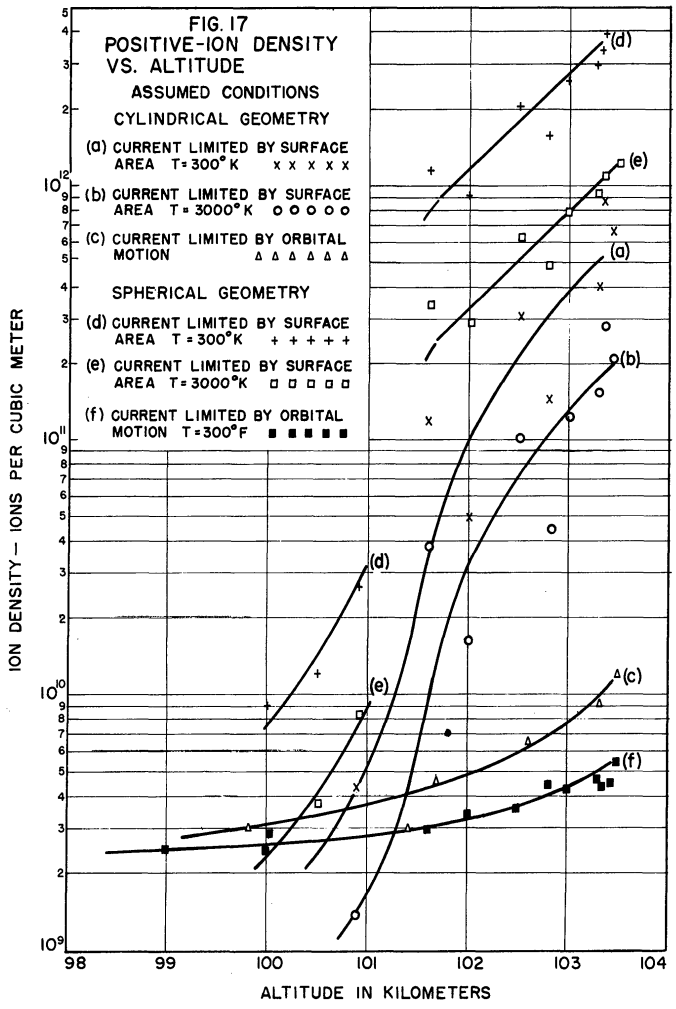

According to Fig. 3 the transition between orbital-motion-limited current and sheath-area-limited current in an ideal cylindrical geometry takes place when

$$\frac{T_p}{N_p r^2} = .71 \times 10^{-4} \tag{67}$$

For T_p = 300°K and r = 6 cm the critical ion density is 1.2 x 10^9; it is ten times larger at 300°K. We should expect that the density-vs.-altitude curves calculated under the assumption of orbital-motion-limited current and sheath—area-limited current, respectively, should intersect approximately at this critical density, where one solution is just as much in error as the other. The data do not confirm this very well; the intersections occur at densities 3 to 5 times higher. This could be taken as an indication of higher ion temperature. As we shall see later this is not the most likely interpretation.

In order to get from the data presented in Fig. 17 an estimate of the positive-ion concentration in the undisturbed E-layer, we should first select the curves in this diagram that are likely to give the best approximation of the sheath-edge ion concentration and then make the appropriate correction for the drop in concentration in the ambipolar diffusion region. When the sheath is very thin, the curve for a cylindrical probe at 300°K is undoubtedly the best one. For larger sheath-thickness the spherical-probe curve for 300°K may be a better approximation. At lower altitudes the sheath-edge ion concentration can be expected to approach the values given by the curve for an orbital-motion-limited probe. As pointed out above, this curve appears to give a somewhat too high concentration of positive ions. This may be caused by a variation of the effective solid angle of the spherical, or rather conical, flow to the probe. If this angle increases when the probe sheath increases relative to the rocket sheath, the slope of the probe curve for negative probe voltage would be increased, thus giving too high positive-ion concentration when the ideal spherical probe relation (Eq 41) is used for computation of ion concentration.

Because of the short length of the probe we are justified in using the spherical solution of the ambipolar diffusion to estimate the drop in the positive-ion density from free space to the sheath edge. At the altitude of 103.5 km the radius of the sheath of the small collector was about 10 cm, and consequently $N_{po} \approx 1.25\ N_a$. This is probably too low; despite its elongated shape the rocket itself is bound to modify the flow of ions in the diffusion region. An oppositely extreme value can be computed by considering the rocket equivalent to a sphere with the same area. Its radius would be 1.6 m and its sheath radius slightly larger, say 1.75 m. Then $N_{po} \approx 4.6\ N_a$. The actual value is probably between 1.5 and 2.

The described process of selecting the most plausible values from Fig. 17 and applying a rough correction for ambipolar diffusion leads to the estimated positive-ion concentration shown in Fig. 18. At the highest altitude a correction factor of 1.5 to 2 has been applied to account for the drop caused by diffusion. This factor has been increased slowly as the altitude is reduced. At the low end the concentration approaches asymptotically a curve somewhat lower than curve f in Fig. 17.

It is interesting to compare these preliminary results of ionospheric probe measurements with the electron densities and E-layer altitudes determined by radio-propagation tests. The ionosphere recorders at White Sands, New Mexico, at 2:30 p.m. on December 8, 1947, i.e., at the time and place of the rocket firing, indicated an E-layer virtual height of 110 km and a corresponding critical frequency of 3.4 mc, or a maximum electron density of 1.45×10^{11} per m^3. This is roughly 1/10

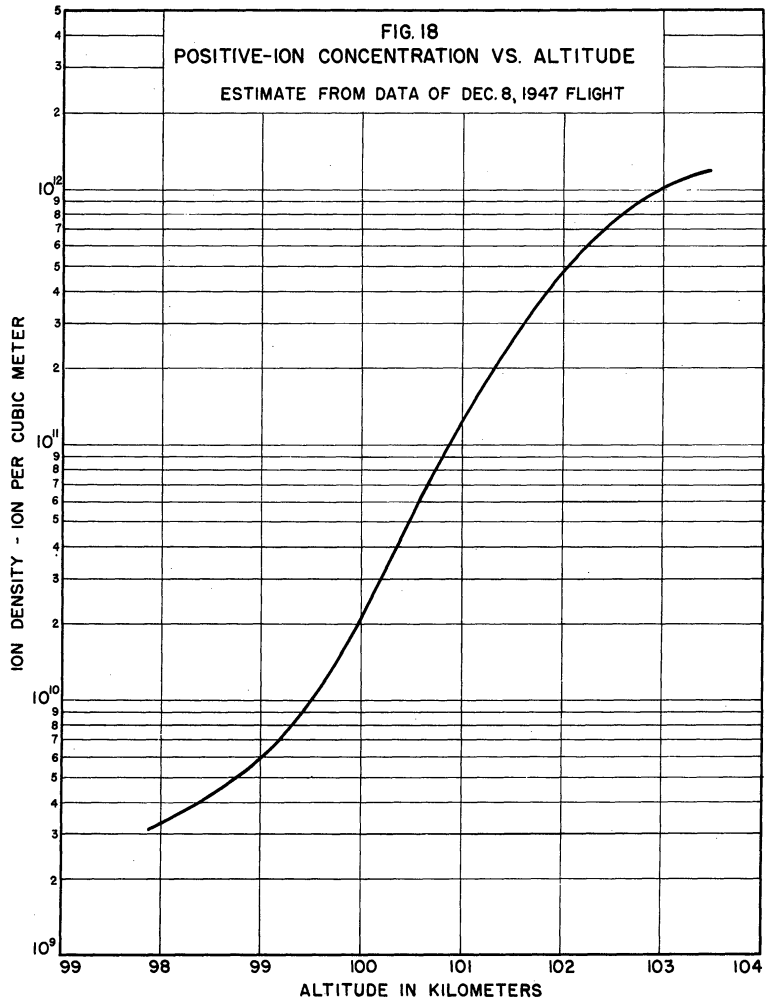

of the maximum positive-ion density obtained from the probe data. Crude as these first probe tests are, careful study of the interpretation makes it seem unlikely that one should discount completely this evidence that either the positive-ion density appreciably exceeds the electron density or the ion temperature is considerably higher than the gas temperature. It has long been assumed that only a negligible number of negative ions, compared to the number of electrons, exist in the E-layer. This assumption has recently been questioned, however, and other evidence for a considerable concentration of negative ions has been reported. It appears, therefore, that the most probable explanation of the discrepancy between

the anticipated and the observed concentration of positive ions is an unexpected abundance of negative ions.

In this analysis the motion of the rocket relative to the air has been disregarded. Actually the rocket had a velocity component perpendicular to its axis of about 150 m/sec. Since the mean thermal velocity of the positive ions is about 390 m/sec, the relative motion is not negligible, but it is a minor factor in comparison with the uncertainties introduced by the imperfect geometry, the limited accuracy of the diffusion theory, etc.

The positive-ion-concentration data from the descent differ rather radically from those recorded during the ascent. This fact will be discussed later in connection with other anomalies of the probe characteristics for the descent.

C. Positive Probe Current and Electron Energy.

The part B-C of the volt-ampere characteristics of an ideal probe (Fig. 8) can be separated into a positive-ion-current curve and a negative-particle-current curve, as pointed out in an earlier section (page 20). A plot of the logarithm of the current vs. the probe potential is in case of temperature equilibrium a straight line with a slope inversely proportional to the temperature (Eq. 29).*

* Johnson and Malter[17] have criticized the discussion of electron energy included in a preliminary publication of some material connected with the present report.[19] Their criticism is largely justified as far as the authors' speculation about a non-Maxwellian velocity distribution is concerned. Even with a Maxwellian distribution the log i_e-vs.-V plot could hardly be expected to be linear over so wide a range as that shown in a diagram in the preliminary publication, despite the very large ratio of the collector areas. The main reason, however, is the unfavorable geometry and consequent overlap of sheaths and diffusion zones. If Johnson and Malter mean to imply that a method like theirs would give better results, this is contradicted by the data. The positive part of the probe curve is mostly of such a shape that it is not possible to separate the positive and negative collection components to the large collector with any reasonable degree of certainty.

The probe used on the December, 1947, flight was by no means an ideal one, and these plots do not very well approximate straight lines. Use of the maximum slope close to the foot of the electron-current curve gives an "electron temperature" that varies with altitude as shown in Fig. 19.

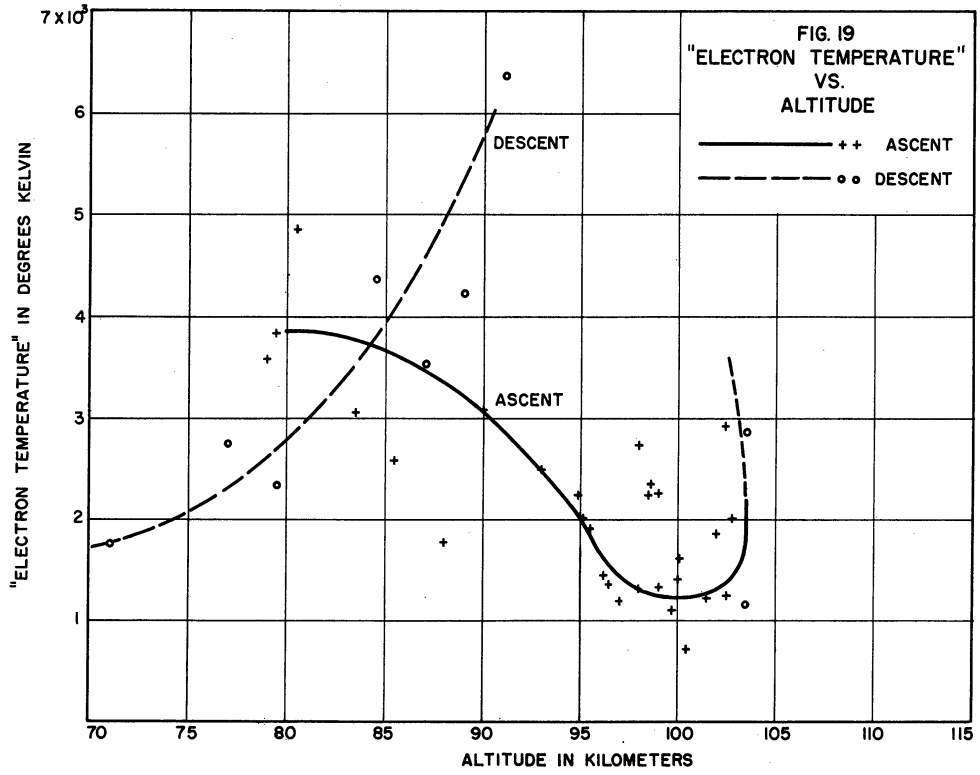

This result differs from the ideally expected one in several important respects. The same temperature should be observed at any specific altitude whether the rocket is ascending or descending, and its value should not differ appreciably from the gas temperature; the temperature equilibrium has been fairly well confirmed by quantitative observations of the "Luxembourg effect". The negative-particle current shows additional peculiarities: at low altitudes it is considerably larger than predicted on the basis of Eq (11) and the positive-ion density calculated in the previous section. The current observed at positive values of δV actually decreases

as the positive-ion density increases (see Figs. 12, 13, 14, 20).

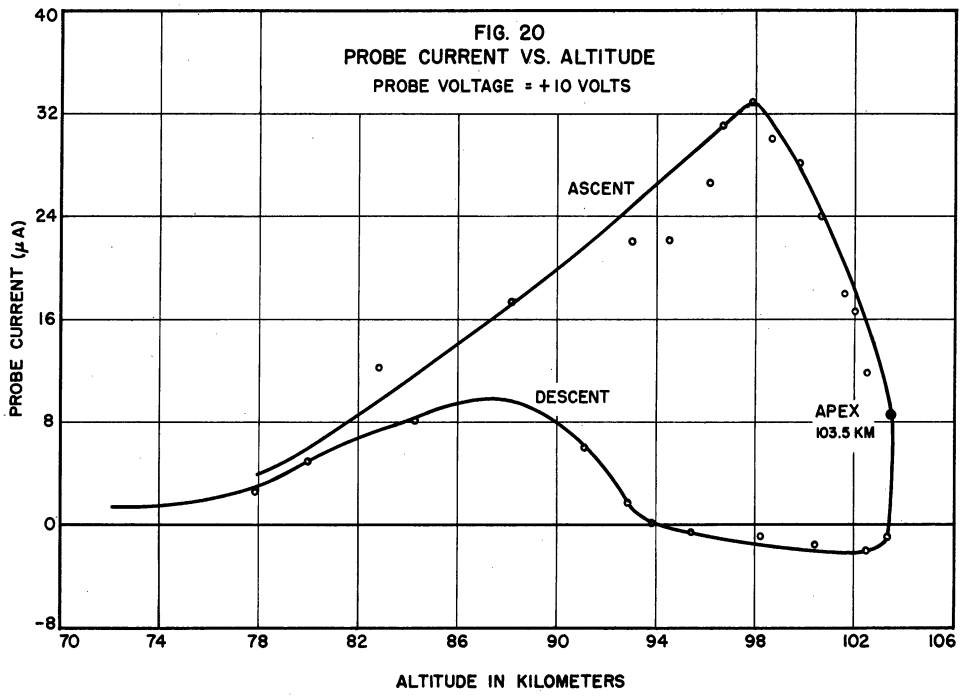

The two main causes of these deviations from the ideal probe theory are believed to be, in addition to the non-cylindrical geometry previously discussed: distortion of the fields and sheaths because of the proximity of the two collectors, and the aerodynamic disturbance caused by the motion of the rocket. The former factor is helpful to explain the results obtained during the ascent; the different behavior during the descent is ascribed to the latter cause. (Fig. 22)

When the ion density is small, so that the sheath thickness is large, the small collector is for a certain range of potentials completely immersed in the sheath of the large collector. As an illustration, Fig. 22 shows a qualitative map of the equipotentials associated with a small electrode close to the surface of a large electrode in the absence of space

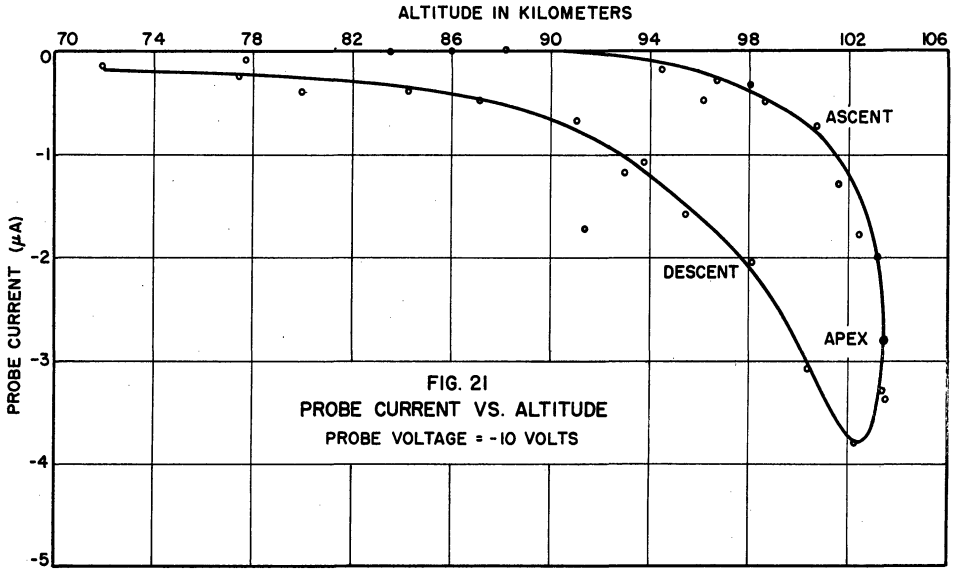

FIG. 21
PROBE CURRENT VS. ALTITUDE
PROBE VOLTAGE = -10 VOLTS

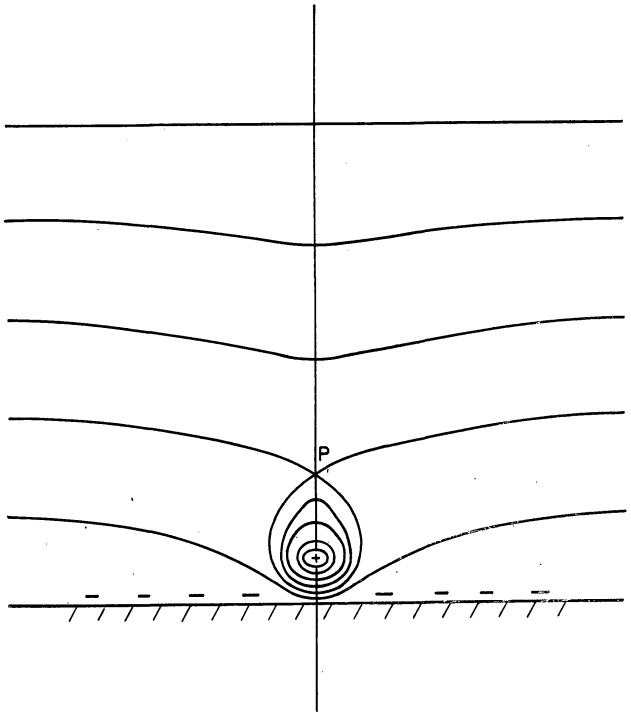

FIG. 22
SKETCH OF A SADDLE-POINT FIELD

charge. If the large electrode has a negative potential with respect to space, and the potential of the small electrode is positive or closer to the space potential, the potential has a "saddle point" (P) outside the small electrode, so that an electron reaching this electrode must have passed through a potential minimum. Whether or not an electron will reach the small electrode depends on the depth of this minimum rather than on the electrode potential. Under such conditions Eq. (11) does not give the collector current. Because of the accelerating field inside the potential minumum a very large fraction of all electrons that penetrate the minimum will reach the electrode. The number of electrons exposed to this accelerating field will be proportional to the "effective area" of the potential minimum. The negative potential of the large electrode, in other words, has the effect of focusing the electrons on the small electrode. This is a possible explanation to the observed electron currents that at the lower altitudes are considerably larger than predicted from Eq. (11). Since the potential at the minimum varies more slowly than in direct proportion to the potential of the small electrode, the plot of log i_e vs. collector potential will give too small a slope and too high an apparent temperature. As the altitude increases, the sheath thickness decreases, and the errors produced by interactions between the sheaths become negligible. Even at the highest altitude attained by this rocket the value of the "electron temperature" calculated from the data is higher than expected, about 1000°K instead of about 300°K. An error of this magnitude could, however, very well be introduced in the calibration and in the process of reducing the data. The resistance of the current-measuring circuit is appreciable, and the correction of the slope for this instrumental error

consequently involves taking the difference between approximately equal numbers with considerable loss in accuracy as a result (see Appendix II). These first crude measurements by means of a bipolar probe thus neither confirm nor contradict the electron temperatures calculated from other observations, although the method certainly is potentially capable of a much more accurate answer than so far obtained.

The rocket had a considerable horizontal velocity component; close to the apex of the trajectory the motion was consequently nearly horizontal, and the air surrounding the probe was violently disturbed. Just beyond the apex the ionization gauge on the axis as well as one of the side gauges read a pressure lower than that read by the other gauges by a factor of ten. The correlation between the anomalous probe characteristics (Fig. 14) and this disturbance suggests a causal connection. That the correlation is not a coincidence is indicated by the fact that a very similar correlation was observed an appreciable time before the apex of an earlier flight, February, 1947, in this case probably caused by a strong wind hitting the rocket at that moment. That time (Fig. 23) the positive probe current was not completely wiped out as it was in Fig. 14, but the sharp upward bend in the

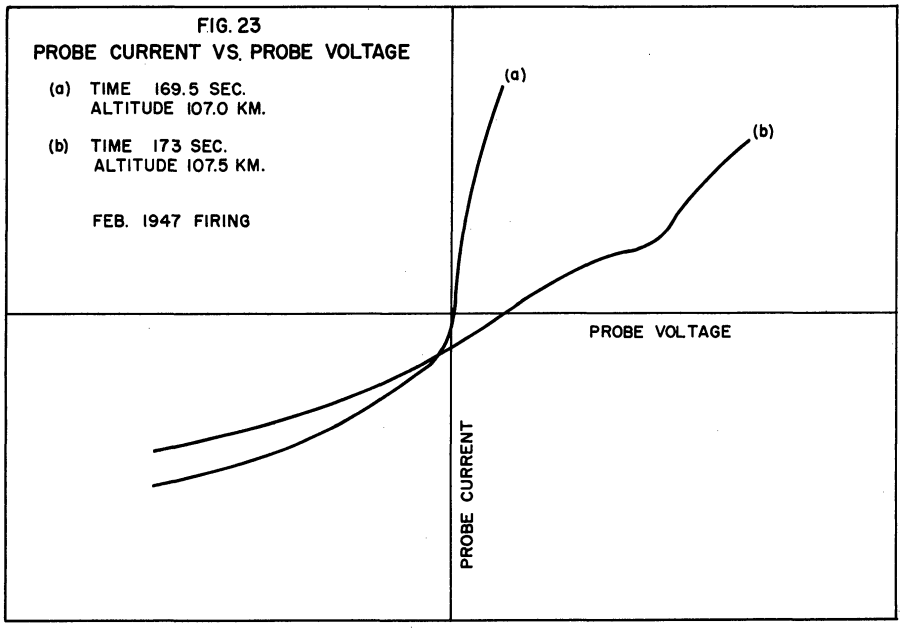

probe curve disappeared and was replaced by a gentle slope. The nose gauge and two of the side gauges showed a sudden drop in pressure, the former by a factor of 10, the latter by factors of 5 and 2, respectively. Evidently the rocket axis was slightly inclined from the vertical, and the wind hit from the tail end. The instantaneous drop in pressures makes it very unlikely that the earlier cavitation on one side of the nose piece as compared to the December 8, 1947 flight was solely due to a different rocket aspect; in contrast the pressure differential between the various gauges about the nose on the December 8 flight formed quite gradually.

The most remarkable fact about the Fig. 14 and Fig. 23 data is the high particle energy involved. In Fig. 14 it is seen that a current is forced through the system against an opposing voltage of up to 20 volts. Temperature rises caused by adiabatic compression or viscous friction in the boundary layer are obviously inadequate to explain energies of this order of magnitude. Local electric fields produced by density gradients or by the rapid flow of plasma through the earth's magnetic field are too small to accelerate the electrons appreciably during a single transit through the field. It is necessary to look for a cumulative process whereby the same electrons are repeatedly exposed to accelerating forces in the same disturbed region. Bohm and Gross have shown that instability phenomena in a plasma may result in a considerable acceleration of a group of electrons.[20] The density gradient of atoms and ions indicated by the large difference between the pressures recorded by closely spaced ionization gauges may be a cause of such instability. Another may be the mixing in the slip stream of the rocket of plasma streams that have followed different paths about the rocket and have different velocities and directions. Violent turbulence in the plasma in conjunction with the earth's magnetic field will produce an

equivalent electric field of random direction and intensity. The viscosity of the air and the magnetic field may keep the same group of electrons long enough in the disturbed region to raise their temperature substantially, in spite of the low intensity of the electric field. The fundamental reason why the electron temperature can rise appreciably above the gas temperature regardless of the frequent collisions of the electrons with gas molecules is of course that the lower concentration of electrons is partly counterbalanced by the smaller mass of the electron and the longer range of the Coulomb electron-to-electron interaction as compared to the electron-to-molecule collision interaction. This enables the aggregate of electrons to retain some of the increase in kinetic energy and gradually to build up their temperature. The electrons accelerated by such processes would make the potential of both collectors more negative with respect to the plasma, thus increasing the positive-ion current above the value observed at the same altitude during the ascent. The geometry of the collectors and the asymmetry of the electron and ion flow may very well explain the fact that the net current to the small collector in Fig. 14 is negative even when this electrode has a higher potential than the other.

During the ascent a similar phenomenon could be expected to occur at the tail of the rocket. Since this part of the rocket was covered with paint it is not too surprising that the probe characteristics do not reveal its presence then.

Alfven has described another mechanism by which charged particles in a plasma can be considerably accelerated.[21] Charged particles that because of their thermal energy describe helical paths along the lines of force of a magnetic field and during part of each loop pass through a stream

that has an appreciable velocity relative to the surrounding plasma may be gradually accclerated by the electric field caused by the polarization of the stream. This process does not seem to fit our case, since it requires a mean free path of the electrons several hundred times the length of one loop of their orbits.

One of the unknown quantities entering the calculation presented here is the ratio of negative-ion to electron concentration. It has been pointed out above that if we accept the assumption of temperature equilibrium a comparison between the positive-ion concentration indicated by the probe data and the electron concentration determined by radio-propagation tests suggests that this ratio is considerably larger than unity. Some qualitative observations may be made regarding this ratio outside the altitude range of reducible data. When the first trace of a probe current appears, at a little more than 60-km altitude, the oscillograms are nearly antisymmetrical; no step indicating electron current is observed. This would mean that the negative charge is carried nearly exclusively by ions. The electron current begins to appear at about 70-km altitude. Similar observations are made during descent; the ion current, however, is larger at the same altitude. Also the electron current is observable to a somewhat lower altitude during descent.

It should be pointed out that the interpretation of the first antisymmetrical probe curves in terms of positive and negative ions is not the only possible one. For instance, photoelectrons emitted from both collectors and collected at a different rate, depending on the difference of potential between the collectors, could possibly give a curve of this type. This interpretation is less probable; the large ratio between the photoemissive areas would upset the antisymmetry. Also, it would have to

be a pure coincidence that this phenomenon occurs suddenly just before the ordinary asymmetric probe curves begin to appear.

CONCLUSIONS

The most important question that this report attempts to answer is whether or not a bipolar probe on a rocket can be so designed that the data obtained will substantially contribute to our knowledge of the atmospheric strata between 60 and 200 km.

We believe that the material presented in this report justifies an affirmative answer. The most questionable point in the reduction of the observed data is the correction for the ambipolar diffusion. In the transition region between the unipolar sheath and the region of ambipolar diffusion neither of the assumptions made in the analysis of these two regions holds. This, of course, affects all probe measurements, and it is not felt that the errors introduced by this circumstance are prohibitive. However, independent experimental determination of diffusion coefficient, mean free path, and volume recombination coefficient is a prerequisite for the accurate reduction of data from the probe measurements.

A detailed discussion of all systematic errors affecting probe measurements in general has been omitted in this report. The subject has been carefully considered and the data have been examined for evidence of their presence. In the present set of data they are certainly small compared to the uncertainties introduced by the imperfect geometry and the interaction between the collectors.

The preliminary exploratory character of the first bipolar-probe experiments does not permit any firm conclusions from the data obtained about the characteristics of the ionospheric E-layer. The negative-particle energy data are not incompatible with an approximate temperature equilibrium.

The positive-ion densities estimated from the data are more likely to be too low than too high; if they are not too high, the positive-ion density exceeds the electron density as measured by radio-propagation methods at least by one order of magnitude. Since it has generally been assumed until quite recently that the ratio of negative-ion concentration to electron concentration is of the order of 0.1 per cent, it would mean that future bipolar-probe tests would be very much worth while for the purpose of settling this question.

The ion density computed from the probe data shows marked random fluctuations with time, but no attempt is at present justified to decide whether this can be altogether attributed to random errors in calibration, telemetering, reading, and reduction of data, or whether it is at least partly caused by passage of the rocket through ion clouds of varying density.

APPENDIX I

PROCEDURE FOR DETERMINING PROBE CURRENT AND VOLTAGE FROM TELEMETERING RECORD

Probe Current

To illustrate the procedure used in reducing the telemetering data, a sample calculation of the probe current will be made. For this purpose, frequent reference will be made to Fig. 24, which shows Channels 3 and 4 of the Telemetering Record No. 1.

Position 2 of Channel 3 is the variable-voltage-probe current, and position 3 is a 3.1-volt calibration voltage. Position 4 is ground. Channel 4 is the variable-voltage-probe current.

In order to measure distances on the telemetering record, a glass plate with a superimposed grid of horizontal and vertical lines was used. The numerical marking of the grid is arbitrary, but the calibration curves were made on the basis of this same system of units.

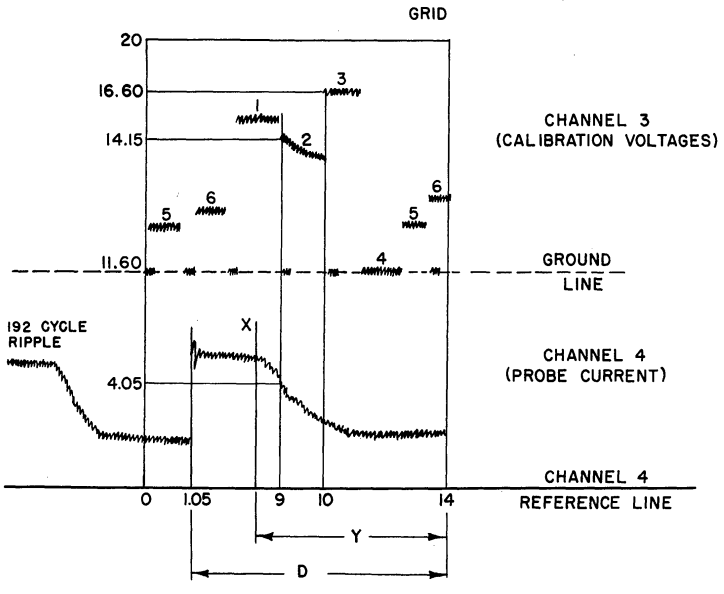

D CORRESPONDS TO. APPROXIMATELY 0.6 SEC.

FIG. 24
SAMPLE OF TELEMETER RECORD

In Fig. 24, the grid is shown in position on the telemetering record at 161 seconds. All straight lines in this figure belong to the grid. The horizontal zero line of the grid is placed on top of the reference line of Channel 4. Vertical grid line No. 14 is placed on the right end of the probe-current pulse in Channel 4. The right end was used as a reference, since it is more sharply defined than the left end, being relatively free of transients.

All vertical distance readings are taken to the average value of the 192-cycle ripple. (This 192-cycle ripple is due to the fact that each of the 23 channels is sampled at a rate of 192 times per second.) Readings are made to the nearest half division of the grid, or 0.05 arbitrary units.

The vertical distance to position 3 (3.1-volt calibration voltage) is found to be 16.60 units. The distance to the ground or zero-voltage pulse is 11.60 units. Thus, 3.1 volts corresponds to 5.0 units in the calibration channel. From the "calibration of Channel 3" curve, Fig. 25, it is seen that 3.1 volts should correspond to 5.3 units.

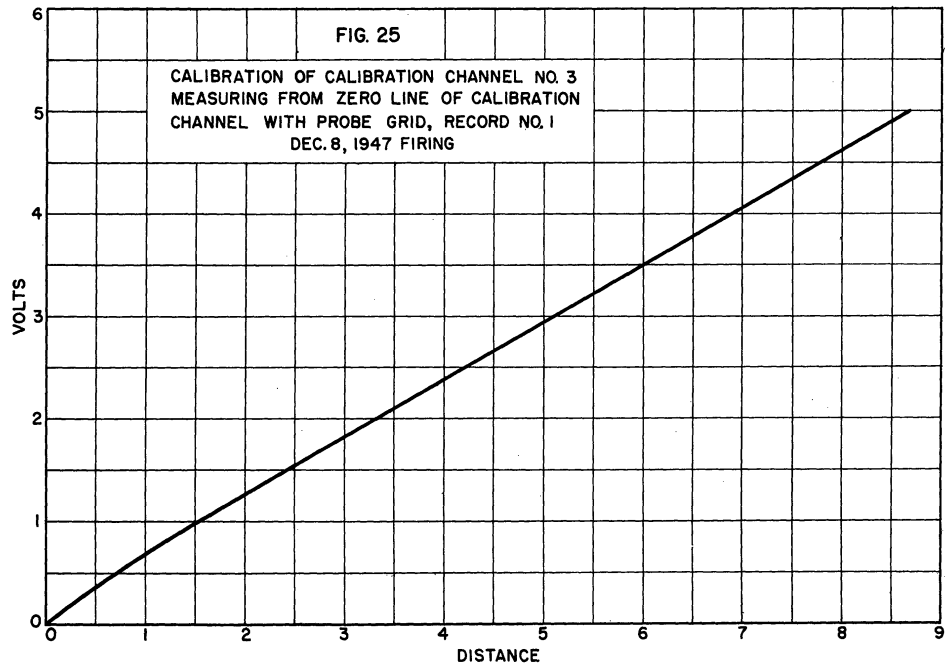

Therefore, distances in the calibration channel are multiplied by the factor 5.3/5.0 to obtain the corrected reading. This, of course, assumes a linear error.

At the horizontal distance 9, position 2, vertical distance is read as 14.15 units. The distance above the ground line is therefore 2.55 units. The corrected distance is then 2.55 (5.3/5.0) = 2.70. From Fig. 25, the corresponding voltage is found to be 1.65 volts.

From Fig. 26, the calibration curve of the probe channel, 1.65 volts is seen to correspond to a distance of 3.95 units. By actual measurement in Channel 4, the distance is found to be 4.05 units. All grid readings must therefore be multiplied by 3.95/4.05 = 0.975 to obtain the corrected reading. Again linear error is assumed.

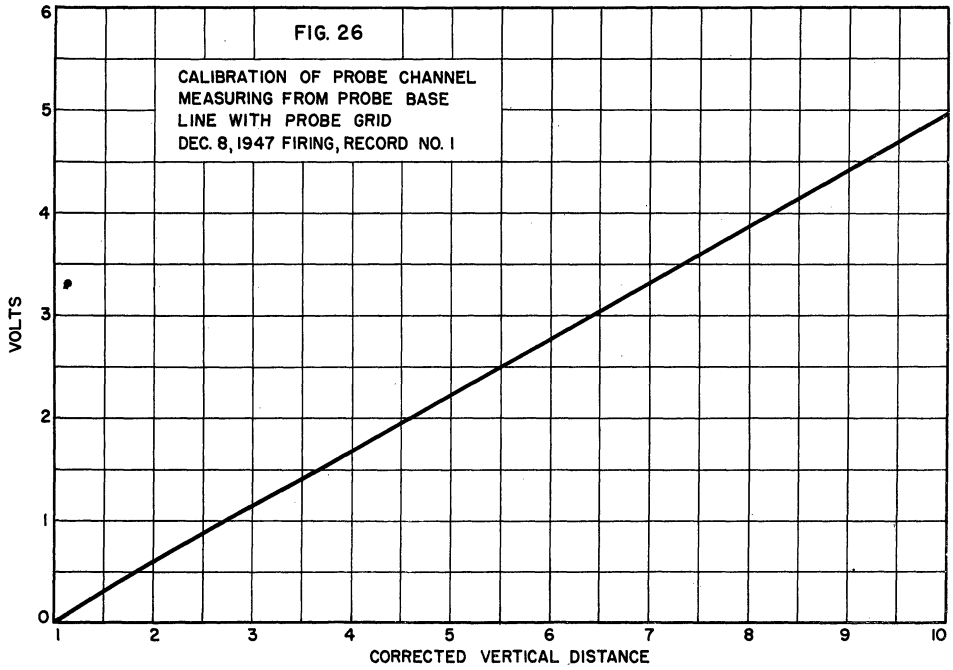

This calibration procedure is repeated at a horizontal distance of 10 units, and for this case the correction factor was found to be 1.00. The average of the two correction factors is then used to correct all the

vertical distances on this cycle. The currents corresponding to these corrected distances are then read from Figs. 27, 28, and 29, which plot vertical distance vs. probe current.

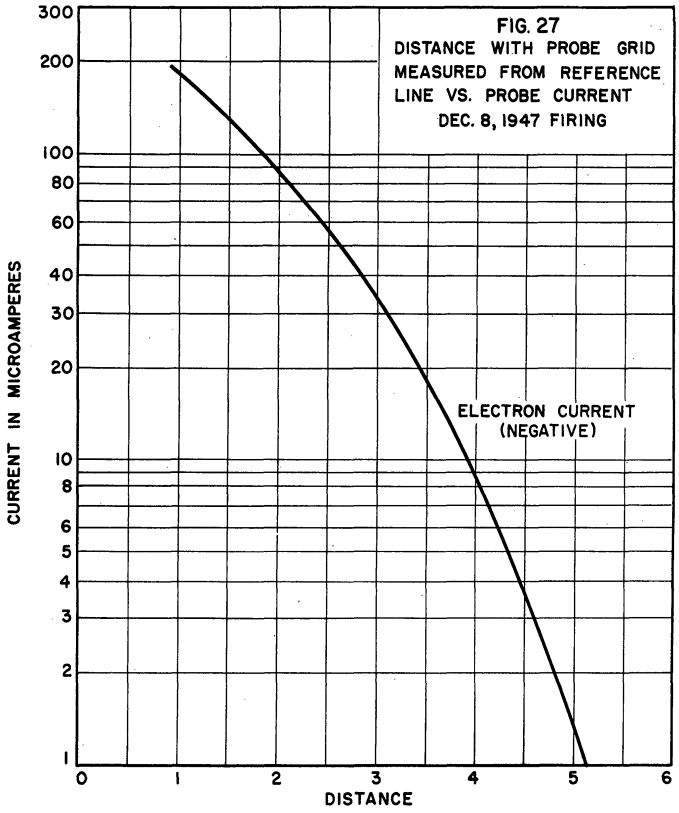

Probe Voltage

The total horizontal length of each cycle D corresponds to a voltage difference of 40.8 volts, from -20.4 to +20.4. The voltage-distance relationship is assumed to be linear. To find the voltage at any point, x, the horizontal grid scale is read at that point. This distance is subtracted from 14, the width of the probe grid, to obtain the quantity y. The length D is taken as the distance from the end of the preceding cycle (1.05 on the grid in this case) to the end of the cycle being measured (14). Then D = 14 - 1.05 = 12.95. The ratio y/D is computed, and the voltage at point x is calculated as $\delta V = (0.5 - y/D)\ 40.8$ volts.

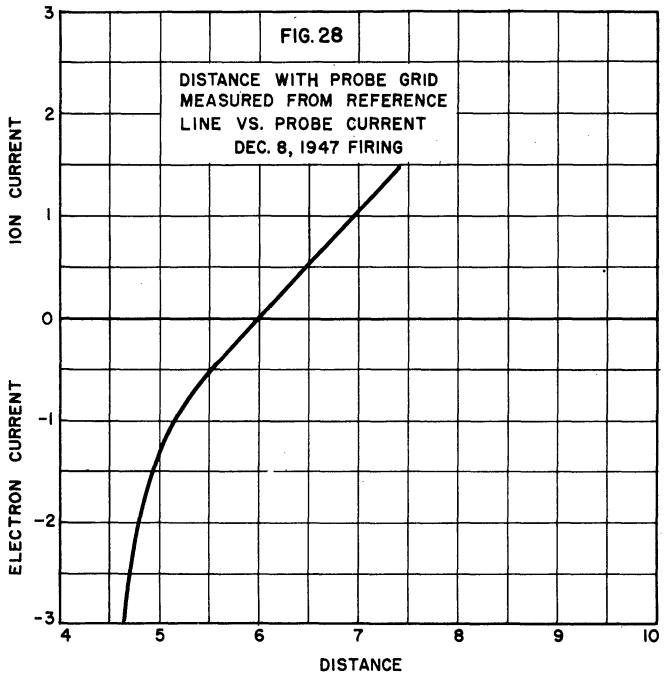
FIG. 28
DISTANCE WITH PROBE GRID MEASURED FROM REFERENCE LINE VS. PROBE CURRENT DEC. 8, 1947 FIRING
ION CURRENT
ELECTRON CURRENT
3
2
1
0
-1
-2
-3
4
5
6
7
8
9
10
DISTANCE

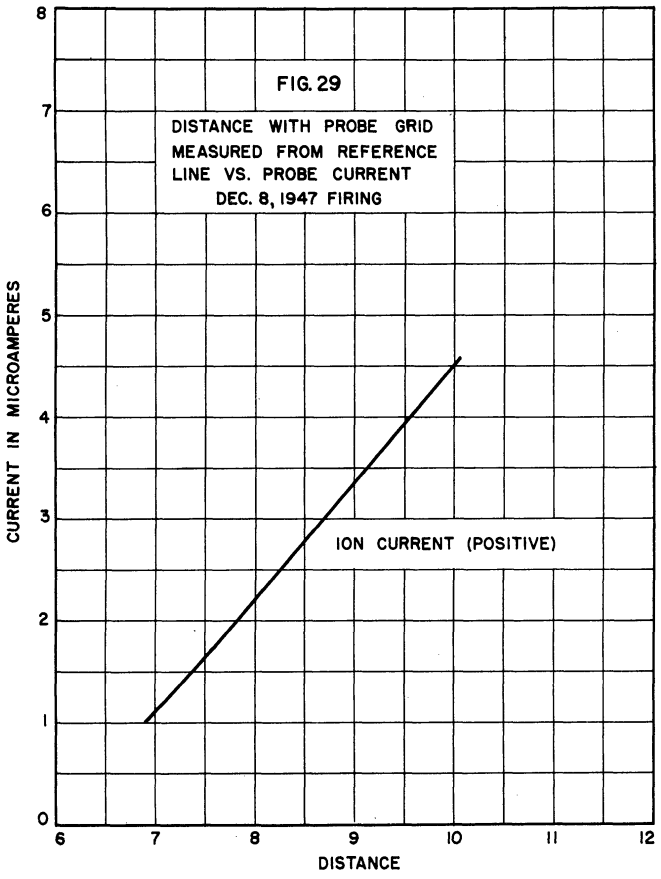
FIG. 29
DISTANCE WITH PROBE GRID MEASURED FROM REFERENCE LINE VS. PROBE CURRENT DEC. 8, 1947 FIRING
CURRENT IN MICROAMPERES
ION CURRENT (POSITIVE)
8
7
6
5
4
3
2
1
0
6
7
8
9
10
11
12
DISTANCE

APPENDIX II

CORRECTION OF PROBE VOLTAGE FOR RESISTANCE IN MEASURING CIRCUITS

The difference in potential between the probe and the missile differs from the potentiometer voltage by the voltage drop across the input of the cathode follower of the measuring circuit. As may be seen from the circuit diagram of Fig. 30, this drop will be dependent on the probe current and the characteristics of the diodes and bias batteries in the range-switching circuit. In the preflight calibration of this circuit, the output voltage was measured as a function of input current, but no measurements were made of the input voltage. Since the equipment was destroyed, no possibility exists to obtain this voltage correction directly, so two alternatives are available. One is to reconstruct the input circuit and measure its voltage drop as a function of input current. However, this method will give results which are extremely dependent on the characteristics of the two range-switching diodes. It

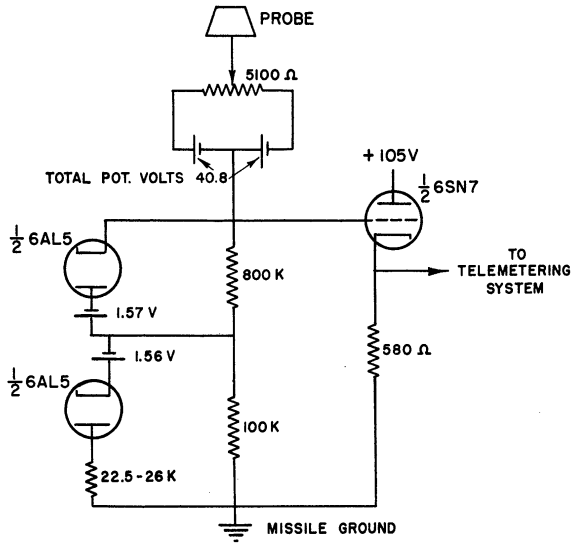

FIG. 30
PROBE CIRCUIT (DEC. 8, 1947 FIRING)

is thought that the actual circuit characteristics can be more accurately reconstructed from the input-current—output-voltage calibration curve and measurements on a reproduction of the cathode-follower stage, for which relatively accurate circuit values were measured at White Sands prior to the firing. These values, including voltages, are indicated in the diagram of Fig. 30.

The cathode-follower stage was set up in the laboratory using the constants given, with a 1-megohm input resistor, and the output voltage vs. input voltage was measured (see Fig. 31). Then, using the input-current-vs.-output-voltage calibration (Fig. 32), an approximate probe-current-vs.-input-voltage-drop characteristic can be determined (Figs. 33 and 34). This is the voltage correction that is applied to the potentiometer voltage.

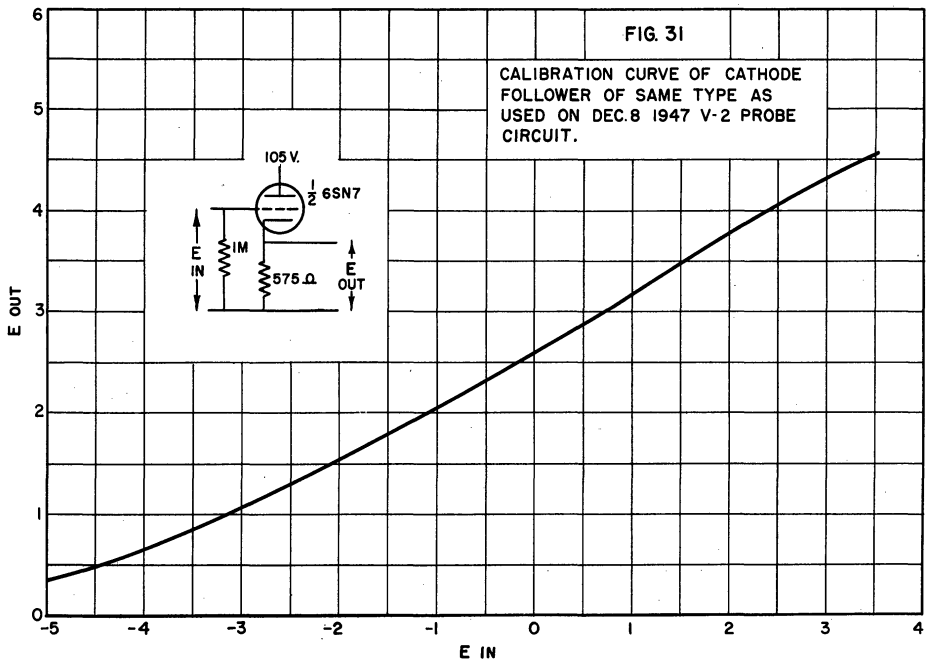

It is observed that the voltage correction has a very noticeable effect on the calculated electron temperature, reducing the temperature as calculated without corrections by a factor of approximately two. The correction also reduces the scattering of the data.

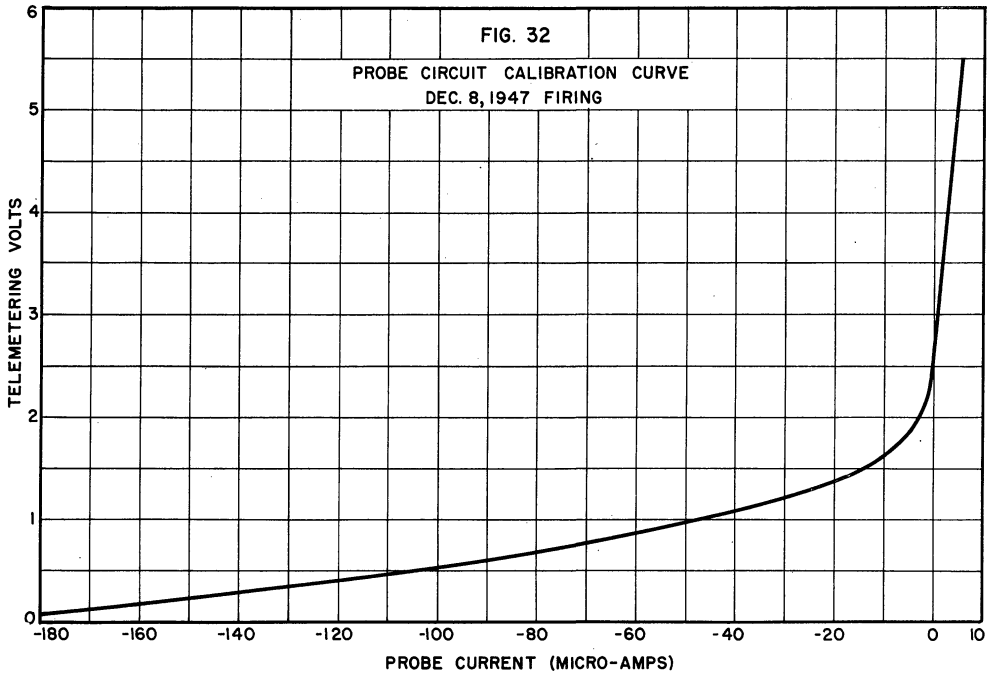
FIG. 32
PROBE CIRCUIT CALIBRATION CURVE
DEC. 8, 1947 FIRING
TELEMETERING VOLTS
6
5
4
3
2
1
0
-180
-160
-140
-120
-100
-80
-60
-40
-20
0
10
PROBE CURRENT (MICRO-AMPS)

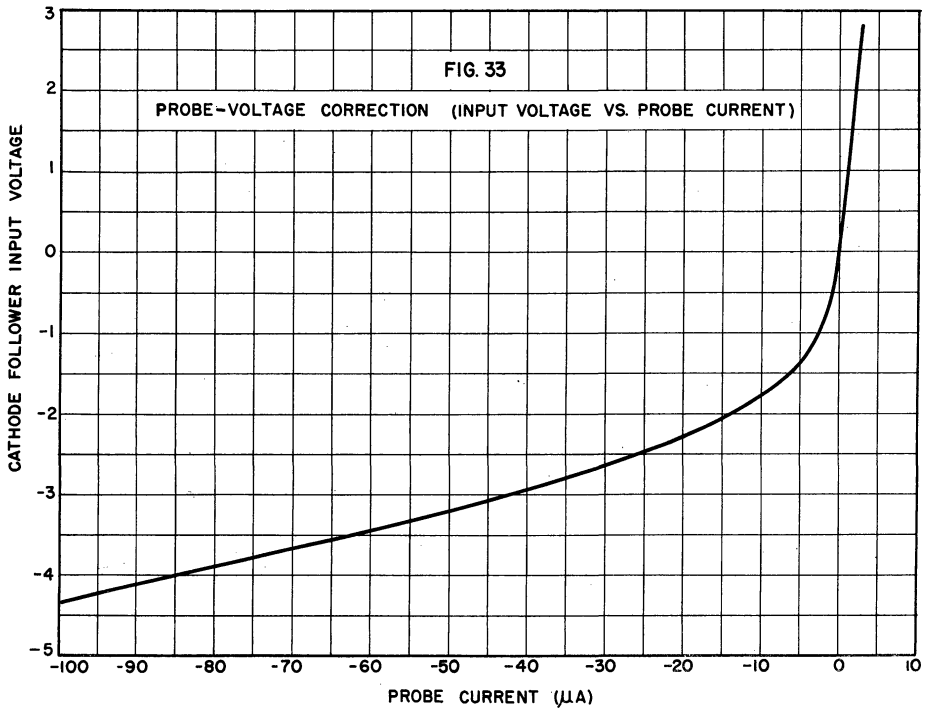
FIG. 33
PROBE-VOLTAGE CORRECTION (INPUT VOLTAGE VS. PROBE CURRENT)
CATHODE FOLLOWER INPUT VOLTAGE
3
2
1
0
-1
-2
-3
-4
-5
-100
-90
-80
-70
-60
-50
-40
-30
-20
-10
0
10
PROBE CURRENT (μA)

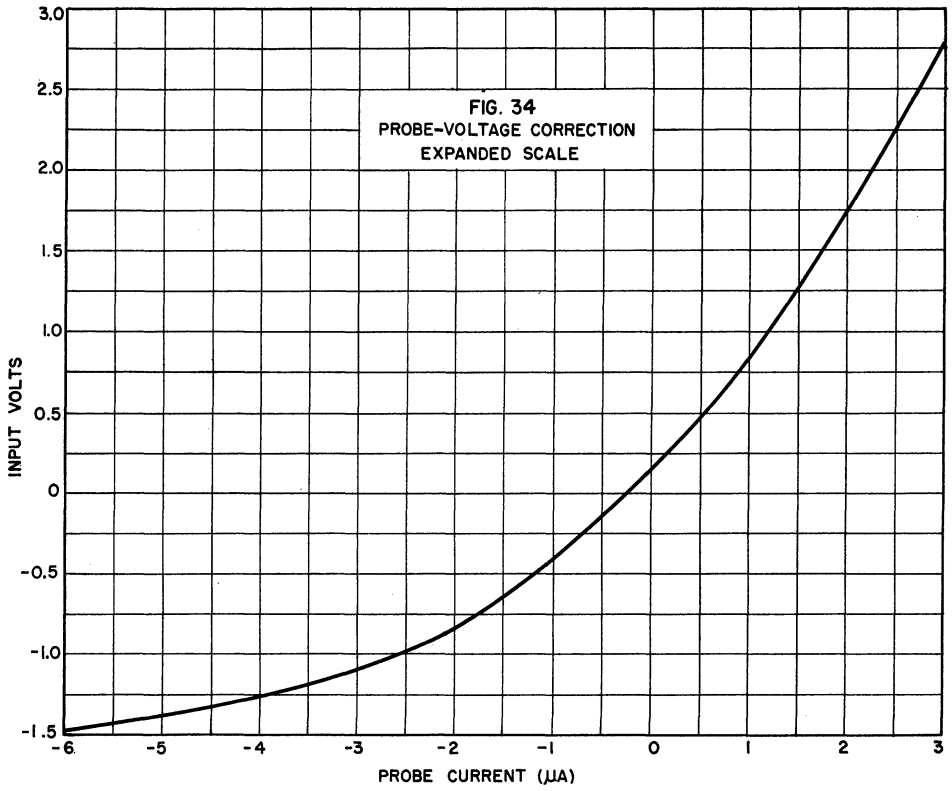
FIG. 34
PROBE-VOLTAGE CORRECTION
EXPANDED SCALE
INPUT VOLTS
3.0
2.5
2.0
1.5
1.0
0.5
0
-0.5
-1.0
-1.5
-6
-5
-4
-3
-2
-1
0
1
2
3
PROBE CURRENT (μA)

APPENDIX III

THE FIRST TENTATIVE INTERPRETATION OF THE DATA FROM THE DECEMBER, 1947 FLIGHT

In order to arrive at an agreement between the positive-ion density calculated from the data and the electron density obtained from radio-propagation tests, it was necessary in the discussion of results presented in the main body of this report to assume that the ratio of the density of negative ions to that of electrons was much larger than is generally expected. In an earlier attempt at an interpretation of the data[19] this agreement was reached by giving up the idea of an approximate temperature equilibrium in the E-layer and ascribing relatively high energies to the ions and electrons. It was believed that the data gave evidence not only of such energies but also of a non-Maxwellian velocity distribution for the electrons. As pointed out above, it is now the authors' opinion that a number of errors and uncertainties in the experiment were overlooked or underestimated in the first evaluation of the data. For the sake of completeness, the theory on which this early interpretation was based is presented in this appendix.

The goal of this theory was to develop a formula with a sufficient number of parameters and of a suitable functional form so that synthetic volt-ampere curves could be produced identical to those observed. The probe theory based on Maxwellian velocity distributions failed to do so in two respects. The electron current to the small collector did not become observable until the difference of potential between the collectors was about +2 volts, while the Maxwellian theory predicted a few tenths of

a volt. It was also considered that the plots of the logarithm of the observed electron current to the small collector vs. the collector difference of potential were not linear over as wide a range as predicted on the same basis. A velocity distribution characterized by a uniform drift velocity superposed on a Maxwellian velocity distribution was found to give the desired result.

Proceeding from Eq. (2) in the review of the probe theory above, we obtain the following expression for the current to a cylindrical collector for such a velocity distribution of the particles:

$$i = \frac{AI\gamma}{\pi}\int_0^{\pi} d\theta \int_{0,(-\eta)^{1/2}}^{\infty} x \exp\left[-(x - s\cos\theta)^2\right] \left\{ \operatorname{erf}\left[\left(\frac{x^2+\eta}{\gamma^2-1}\right)^{1/2} + s\sin\theta\right] + \operatorname{erf}\left[\left(\frac{x^2+\eta}{\gamma^2-1}\right)^{1/2} - s\sin\theta\right]\right\} dx \qquad (71)$$

The notations are the same as those used previously in this report. The random current density I is now referred to a coordinate system moving with the drift velocity. The dimensionless quantity s is the ratio of the drift velocity to the most probable velocity of the Maxwellian distribution. The drift velocity is assumed to be perpendicular to the axis of the cylinder. θ is the angle between the radius vector and the direction of the drift velocity. The distortion of the sheath from the shape of a cylinder coaxial with the collector is assumed to be negligible. As before, the second integration takes place between the limits 0 to ∞ for an accelerating field and $(-\eta)^{1/2}$ to ∞ for a retarding field in the sheath.

In the case of interest here, the potential of the collector is negative with respect to space, so that a positive-ion sheath is formed.

The positive ions move in an accelerating field, while the electrons meet a retarding field on entering the sheath.

If s = 0, the electron current is the same as previously obtained:

$$i_e = A\, I_e\, e^{\eta} \quad . \tag{72}$$

When the drift is not negligible, an asymptotic expression for Eq. 71 can be obtained by letting γ approach infinity. This case was considered in detail by Langmuir when, in addition, the drift parameter s is approximately equal to or greater than $\sqrt{-\eta}$, the result can be expressed in the following form:

$$i_e = 0.384\, A\, I_e\, \sqrt{s}\, F_1(\lambda) \quad , \tag{73}$$

where

$$\lambda = s - \sqrt{-\eta} \tag{74}$$

$$F_1(\lambda) = \frac{2}{\Gamma(3/4)} \int_0^{\infty} \sqrt{x}\; e^{-(x-\lambda)^2}\, dx \tag{75}$$

Here, as in Eq. 72, the current collection in a retarding field is independent of the sheath thickness.

When the collector radius is large and the sheath thickness is moderate or small, a different asymptotic solution is helpful. If γ approaches unity, Eq. 71 becomes

$$i_e = A\, I_e \left\{ e^{-\lambda^2} + s\sqrt{\pi}\; \mathrm{erf}(-\lambda) \right\} = A\, I_e\, F_2(\lambda, s) \quad , \tag{76}$$

valid for $\sqrt{-\eta} > s > 1$.

Eqs. 73 and 76 show that, when the electrons have an appreciable drift velocity, a plot of log i_e vs. the collector potential or η_e cannot be expected to be a straight line as it is when Eq. 72 holds. To demonstrate this, the graph in Fig. 35 presents the logarithm of the right-hand side of Eq. 73 vs. η_e for various values of the drift parameter s. For large retarding potentials, the curves are approximately linear, but the slope is considerably smaller than when the drift is zero. Interpreted on the basis of Eq. 72, they would be held to indicate a much higher electron temperature than the one actually prevailing.

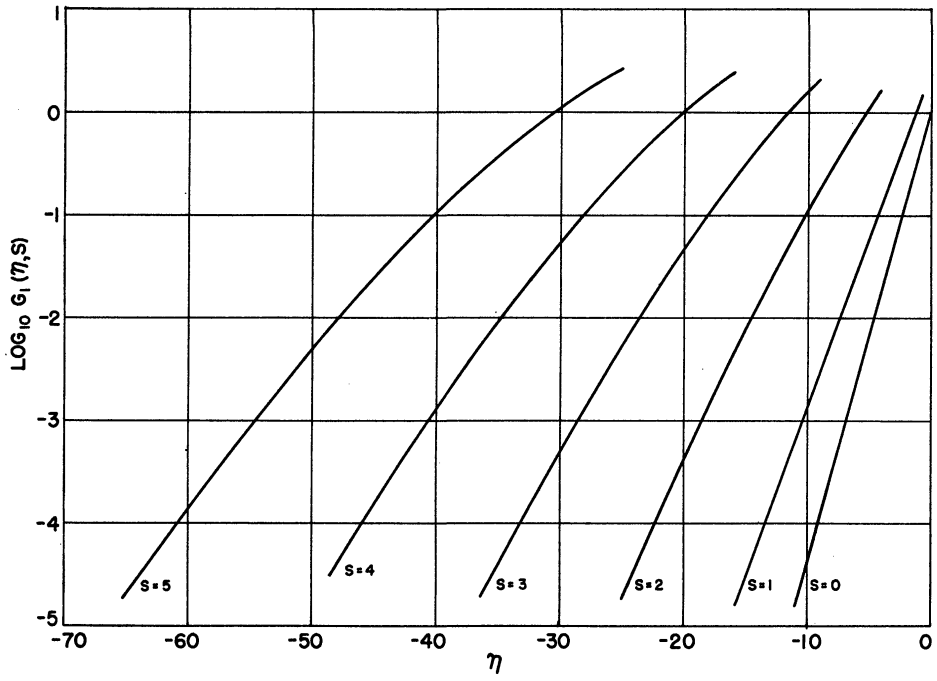

FIG. 35
THE LOGARITHM OF THE ELECTRON CURRENT VS. THE POTENTIAL PARAMETER η

Another observable quantity of interest is the difference in isolation potential between the two collectors, which is represented by the intersection of the bipolar-probe volt-ampere curve with the voltage axis. It is also a function of the temperature and drift velocity of the electrons. Fig. 36 gives the isolation potentials of two cylindrical

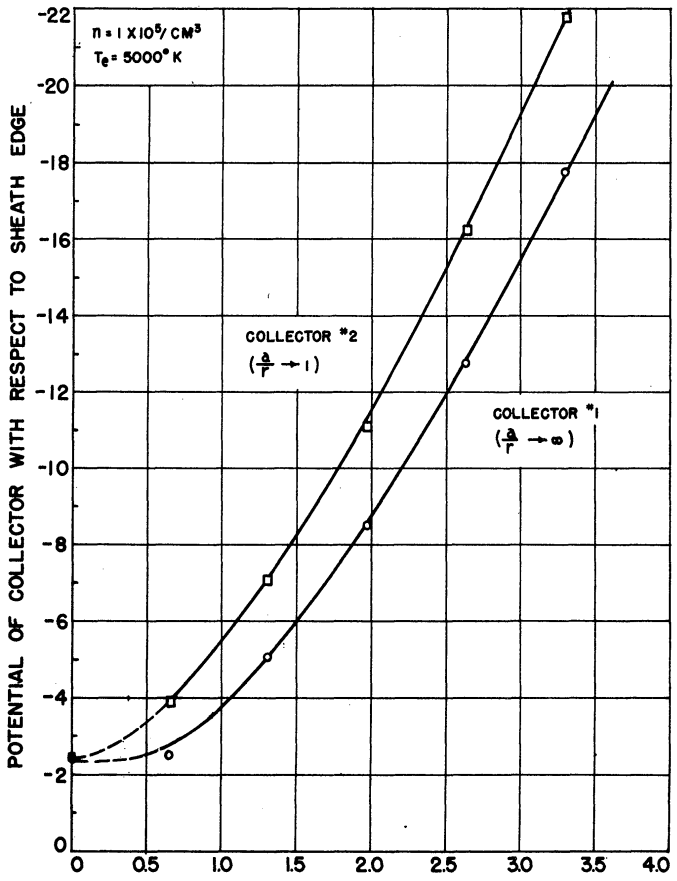

FIG. 36
EQUILIBRIUM POTENTIAL VS. ELECTRON DRIFT VELOCITY

collectors, one of large radius ($\gamma \approx 1$) and one of small radius ($\gamma \approx \infty$), as a function of the electron drift velocity.

In this early interpretation of the data the collectors were assumed to have ideally cylindrical geometry and no interaction between sheaths. The density of negative ions was assumed negligible. The electron current to the small electrode was obtained by extrapolation of the positive-ion current as previously described. The logarithm of the electron current is plotted in Fig. 37 for a few representative altitudes on the ascent. It should be remembered that the data at this point had not yet been corrected for the resistance of the measuring circuit.

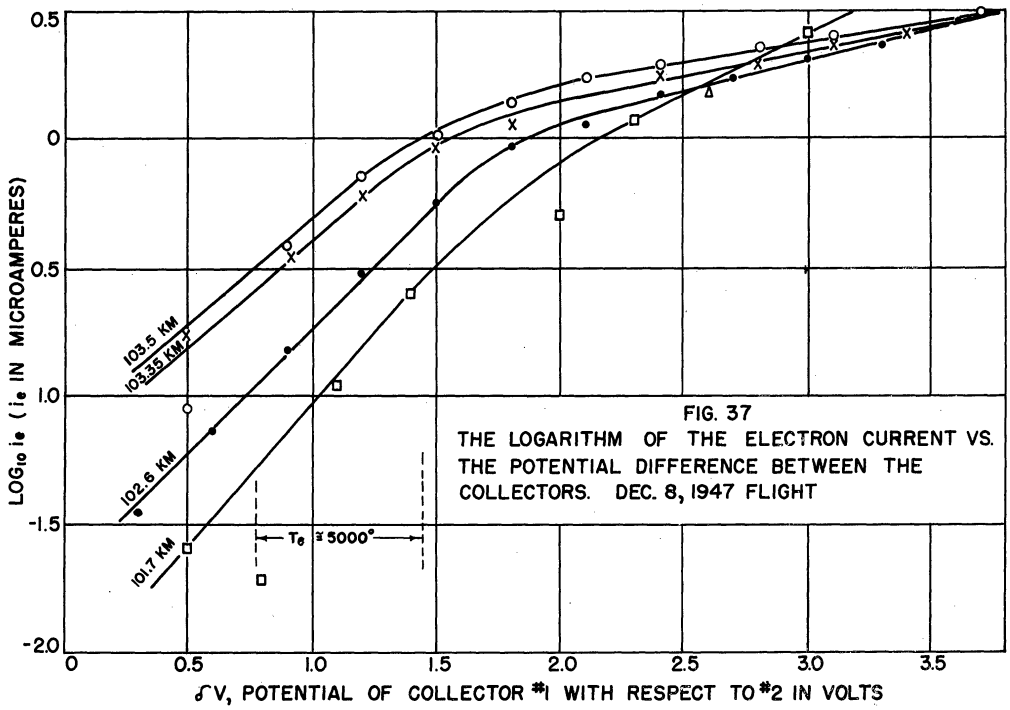

FIG. 37
THE LOGARITHM OF THE ELECTRON CURRENT VS. THE POTENTIAL DIFFERENCE BETWEEN THE COLLECTORS. DEC. 8, 1947 FLIGHT

Due to the transcendental nature of Eq. 73, the drift velocity and the electron temperature have to be found from the data by numerical or graphical methods; for instance, by selecting a pair of values by trial and error, checking them by calculating the electron current at two different collector potentials, and comparing the result with the data. The electron density was taken equal to the positive-ion density determined from the positive-ion current at higher negative collector potential. In this way an electron temperature of 1500°K and a drift-velocity ratio s of approximately 6, or a drift velocity of roughly 1500 km/sec, were arrived at close to the apex of the rocket trajectory. These figures agree also, at least as far as the order of magnitude is concerned, with the observed difference between the isolation potentials of the two collectors.

Incidentally, the sample probe curves shown in Figs. 7 and 8 were calculated from the theory presented above, using the following "model" data: density of positive ions and electrons 10^{11} per m^3; electron temperature

5000°K; electron drift velocity 2 volts$^{1/2}$; area of collector No. 1 0.05 m^2; and area of collector No. 2 0.8 m^2.

This first interpretation of the data from the December 8, 1947 rocket flight was abandoned because the indications supporting it were considered too weak to contradict evidence obtained elsewhere of an approximate temperature equilibrium in the lower ionosphere. The imperfect collector geometry, particularly the overlapping of sheaths and diffusion regions, and the uncertainty in the collector potential caused by contact potentials and imperfections in the potentiometer were the main factors considered.

Furthermore, the assumption of a convection-current density of the order of magnitude consistent with this drift leads to other difficulties. Diurnal variations of the terrestrial magnetic field caused by currents in the E-layer are observable, but of a considerably smaller magnitude. According to the most successful theory, they are produced by "dynamo action" in the earth's magnetic field caused by tidal and thermal motions of the upper atmosphere. The velocity involved in such motions may be an appreciable fraction of the mean thermal velocity, but the accuracy of the bipolar-probe measurements is certainly not at present high enough to justify a correction for such a modest drift motion of ions and electrons.

BIBLIOGRAPHY

1. Tonks, L., "High-Frequency Behavior of a Plasma", Physical Review, 37, 1458 (1931).

2. Mott-Smith, H. M., and Langmuir, I., "Studies of Electric Discharges at Low Pressures", General Electric Review, 27, 449, 538, 616, 762 (1924).

3. Mott-Smith, H. M., and Langmuir, I., "The Theory of Collectors in Gaseous Discharges", Physical Review, 28, 727-763 (1936).

4. Penndorf, R., "The Distribution of Atomic and Molecular Oxygen in the Upper Atmosphere", Physical Review, 77, 561 (1950).

5. Bates, D. R., "Ionization and Recombination Processes in the Upper Atmosphere", Proceedings of the Conference on Ionosphere Physics, Pennsylvania State College, 2, 1S (1950).

6. Sayers, J., "Evidence on Recombination Processes from Laboratory Measurements on Ionized Gases", Proceedings of the Conference on Ionosphere Physics, Pennsylvania State College, 2, 1 K (1950).

7. Ferraro, V. C. A., "Diffusion of Ions in the Ionosphere", Terrestrial Magnetism and Atmospheric Electricity, 50, 215-22 (1950).

8. Johnson, M. H., and Hulburt, E. O., "Diffusion in the Ionosphere", Physical Review, 79, 802 (1950).

9. Mitra, S. M., "A Radio Method of Measuring Winds in the Ionosphere", Journal of Institute of Electrical Engineers, part III, 96, 441 (1949).

10. Symposium on Dynamic Characteristics of the Ionosphere, Proceedings of the Conference on Ionosphere Physics, Pennsylvania State College, 2 (1950).

11. Schultz, F. V., Spencer, N. W., and Reifman, A., "Atmospheric Pressure and Temperature Measurements between the Altitudes of 40 and 110 Kilometers", AMC Cambridge Field Station Upper Air Research Program Report No. 2, Engineering Research Institute, University of Michigan (1948).

12. Newell, H. E., and Stry, J. W., "Upper Atmosphere Research Report No. III", Naval Research Laboratory Report No. R-3120 (1947).

13. Huxley, L. G. H., "A Synopsis of Atmospheric Cross-Modulation", Proceedings of the Conference on Ionosphere Physics, Pennsylvania State College, 2 (1950).

14. Langmuir, I., and Blodgett, K., "Currents Limited by Space Charge Between Coaxial Cylinders", Physical Review, 22, 347 (1923) and "Currents Limited by Space Charge Between Concentric Spheres", Physical Review, 24, 49 (1924).

15. Dow, W. G., Fundamentals of Engineering Electronics, Wiley, New York 1937.

16. Loeb, L. B., Fundamental Processes of Electrical Discharges in Gases, Wiley, New York, 1939.

17. Johnson, E. O., and Malter, L., "A Floating Double-Probe Method for Measurements in Gas Discharges", Physical Review, 80, 58 (1950).

18. Reifman, A., and Dow, W. G., "Theory and Application of the Variable-Voltage Probe for Exploration of the Ionosphere", Physical Review, 75, 1311A (1949).

19. Reifman, A., and Dow, W. G., "Dynamic-Probe Measurements in the Ionosphere", Physical Review, 76, 987 (1949).

20. Bohm, D., and Gross, E. P., "Theory of Plasma Oscillations", Physical Review, 75, 1851 (1949).

21. Alfven, H., Cosmical Electrodynamics, Clarendon Press, Oxford, 1950.